August 2007

Structural Basis of Allosteric and Intrasteric Regulation in Human Cystathionine β-Synthase and its Regulation by a CXXC Motif

Suvajit Sen

University of Nebraska-Lincoln, sseni@bigred.unl.edu

Structural Basis of Allosteric and Intrasteric Regulation in Human Cystathionine β-Synthase and its Regulation by a CXXC Motif

By

Suvajit Sen

A Dissertation

Presented to the Faculty of

The Graduate College at the University of Nebraska

In Partial Fulfillment of Requirements

For the Degree of Doctor of Philosophy

Major: Biochemistry

Under the Supervision of Professor Ruma Banerjee

Lincoln, NE

June, 2007

Structural Basis of Allosteric and Intrasteric Regulation in Human Cystathionine β-Synthase and its Regulation by a CXXC Motif

Suvajit Sen

University of Nebraska, 2007

Advisor: Ruma Banerjee

The human cystathionine β-synthase (CBS) is a 5' pyridoxal phosphate (PLP) dependent protein that catalyzes the condensation reaction between serine and homocysteine to yield cystathionine. This is the first step in the transsulfuration pathway which connects the methionine cycle to cysteine production. Mutations in CBS are the single most common cause of severe hereditary hyperhomocystenemia and over one hundred pathogenic mutations have been described so far. These mutations represent residues which are important for the structural and functional integrity of the enzyme. The biochemical characterization of these mutants thus leads to further insights into structure-function correlations in CBS.

CBS has a subunit mass of 63 kDa and is a modular protein with 551 amino acids. The N-terminal half of the protein houses the two cofactors, PLP and heme and a CXXC motif comprised of residues C272 P273, G274 and C275. This motif is also found in the thioredoxin family of proteins where it is involved in thiol disulfide exchange reactions. The heme, which is coordinated by the axial ligands H65 and C52, is about 20 Å away

from the CXXC motif as well as the PLP catalytic center. As such, heme does not contribute directly to catalysis, but is believed to be a center for redox regulation in CBS.

The C-terminal half of the protein comprising residues 413 to 551 bear a tandem repeat of "CBS domains," which are secondary structural motifs found in diverse families of proteins with no sequence similarities. In CBS, these domains are believed to be involved in the binding of the allosteric activator S-adenosyl methionine (AdoMet). Along with being involved in allosteric regulation, the C-terminal domain of CBS imposes intrasteric regulation on the catalytic core. Thus deletion of the C-terminal regulatory domain leads to the formation of a super-active enzyme, CBS-ΔC143 which has a 4-fold higher k_{cat} than the full-length protein. It is also known that a truncated form of CBS is generated in cells exposed to proinflamatory agents such as TNFα. Although this observation suggests that the C-terminal domain interacts with the N-terminal catalytic core to effect this regulation, so far no experimental results were available which would characterize the nature of this interaction. In other words no information was available regarding the conformational changes associated with the allosteric and intrasteric regulation in CBS.

In this study, we have mapped the regions of intrasteric and allosteric regulation in CBS. We have employed hydrogen/deuterium (H/D) exchange, mass spectrometric technique to locate conformational changes in the enzyme upon the binding of its allosteric activator, AdoMet. We have also used this approach to detect the surface involved in the interaction of the C-terminal domain with the catalytic core relevant to intrasteric regulation. A change in the kinetics of H/D exchange was located in a single peptide, extending from residues 511-531 upon AdoMet binding. CBS-D444N a patient

mutant exhibits a similar change in the above peptide in its native state and thus samples a conformation which is acquired by the wild type upon AdoMet binding. Accordingly this mutant is not responsive to any further activation by the allosteric activator. Peptides 356-370 and 371-385 in the N-terminal half of the protein exhibited a change in H/D exchange kinetics when the full-length and its counter part in CBS-ΔC143, were compared by H/D exchange studies, associating this region with intrasteric regulation. We have also demonstrated that in addition to heme, the CXXC motif in CBS is a center for redox regulation. Thiol alkylation followed by mass spectrometric analysis demonstrated formation of an intramolecular disulfide bridge between C272 and C275, and identified the presence of a sulfenic acid intermediate under air oxidized conditions in CBS-ΔC143. The full length and the CBS-ΔC143 enzyme exhibited a 1.6 and 4.5 fold enhancement in specific activity respectively upon reduction of their disulfides at the CXXC center. A redox potential of -240 ± 4 mV was determined for the CXXC center using MAL-PEG for titrating thiol content at various ratios of oxidized and reduced dithiotreitol.

Acknowledgement

I am grateful to my advisor, Prof Ruma Banerjee for giving me a chance, bearing with me and lending me her continuous support throughout my graduate career. I am thankful to Prof Steve Ragsdale, for his support and advice during my graduate studies. I would also like to thank Dr Mark Wilson, Dr Joseph Barycki, and Dr Liang-cheng Du, for serving and advising in my committee. I would like to thank Dr Ashraf Raza and Dr Jiong Yu for their sincere help with mass spectrometry. I would like to thank all my colleagues, especially Dr Mamoru Yamanishi for his countless support during preparation of manuscripts. Last but not least I am enormously grateful to my parents whose blessings have made everything possible.

This thesis is dedicated to my grandmothers Mrs Sulata Sen and Mrs Suprava Bose, my parents, Dr Asoke Sen and Mrs Indrani Sen and my friends Brindusha and Raghunath.

Table of Contents

Chapter1

Introduction

1.1 Toxicity of homocysteine

Homocysteine is a non protein sulfur containing amino acid formed during the metabolism of an essential amino acid methionine. Carson and Neil independently described the first error in methionine metabolism by demonstrating an excessive urinary excretion of homocysteine in children who had a deficiency in CBS activity (5). Following this, it was also reported that children with homocystinuria, an autosomal recessive condition showed signs of cardioavascular disorders (35). This lead Dr. Kilmer Mc Cully to suggest a correlation between high levels of homocysteine and cardiovascular diseases (26, 35). Studies over the last twenty-five years have shown that even, mild elevation of homocysteine in the plasma is an independent risk factor for occlusive arterial disease, venous thrombis and vascular causes of mortality (26). More than fifty percent of patients with stroke and/or other cardiovascular diseases have homocysteine levels outside the normal range, which is around 10-15 μM for men and 6-10 μM for women. High levels of homocysteine, are also correlated with several other diseases such as neural tube defects and Alzheimer's diseases (20, 36).

1.2 Role of cystathionine β-synthase in metabolism

Cystathionine β-synthase [EC 4.2.1.22: CBS], is a heme protein and catalyzes the pyridoxal 5'- phosphate (PLP)-dependent condensation of serine and homocysteine to form cystathionine (63). CBS catalyzes the only reaction that irreversibly removes the toxic metabolite, homocysteine, from the methionine cycle. This is followed by the action of a second PLP dependent enzyme, cystathionine γ-lyase which catalyzes the

hydrolysis of cystathionine to α-ketoglutarate and cysteine, a precursor of the major cellular redox buffer, glutathione. Thus CBS catalyzes the first committed step in the transulfuration pathway. Homocysteine, a non-protein sulfur containing amino acid occupies a key biochemical intersection in the methionine cycle between S-adenosyl methionine (AdoMet), the indispensable and ubiquitous methyl group donor in various biological reactions. Homocysteine metabolism is thus regulated to strike a balance between the methylation and transulfuration pathways and to maintain low levels of this toxic metabolite (13).

1.3 Regulation and homocysteine metabolism

Homocysteine is an intermediate in methionine metabolism and is cleared via one of two pathways: the remethylation pathway which regenerates methionine by transfer of a methyl group to homocysteine, and the transsulfuration pathway that degrades homocysteine into cysteine (Fig1.1). Remethylation of homocysteine to methionine is catalyzed by one of two zinc enzymes, cobalamin–dependent methionine synthase (MS) and betaine homocysteine methyl transferase. Another important enzyme in the remethylation pathway is methylenetetrahydrofolate reductase (MTHFR) that generates methyl tetrahydrofolate, the methyl group donor for the methionine synthase–catalyzed reaction. Although both MS and betaine homocysteine methyl transferase, catalyze the remethylation of homocysteine betaine homocysteine methyl transferase has limited tissue distribution being present mainly in the liver and kidneys (19), whereas MS is ubiquitous.

AdoMet, a ubiquitous methyl donor in various metabolic reactions including RNA, DNA, lipid and protein methylations and a precursor of polyamines, is synthesized by adenosylation of methionine catalyzed by methionine adenosyltransferase. AdoMet is demethylated by a variety of methyl transferases to give S-adenosyl homocysteine, which in turn is hydrolyzed to give adenosine and homocysteine catalyzed by S-adenosyl homocysteine hydrolase.

Homocysteine is at a branch point in methionine metabolism. In liver cells, approximately half of the total homocysteine formed is remethylated back to methionine and half is committed to the transsulfuration pathway (16) for the synthesis of cysteine. The transulfuration pathway also provides a route for the disposal of excess sulfur via cysteine catabolism. The flux of homocysteine through the complex pathways is tightly regulated. One regulatory switch between methionine cycle and transulfuration pathway is AdoMet (14). At high concentrations of AdoMet, remethylation of homocsyteine to methionine is inhibited (15, 60). High concentrations of AdoMet signal methionine sufficiency and represses remethylation by inhibiting MTHFR, the source of methyl tetrahydrofolate, the methyl donor in the reaction catalyzed by methionine synthase. Under the same conditions, CBS is activated by AdoMet which increases flux of homocysteine through the transulfuration pathway. It is estimated that ~ 50% of cysteine in the intracellular glutathione pool is derived from homocysteine via the transulfuration pathway in liver cells (43, 61). Thus, regulation at the level of CBS directly controls the removal of homocysteine from the methionine cycle, thereby influencing glutathione-based redox homeostasis.

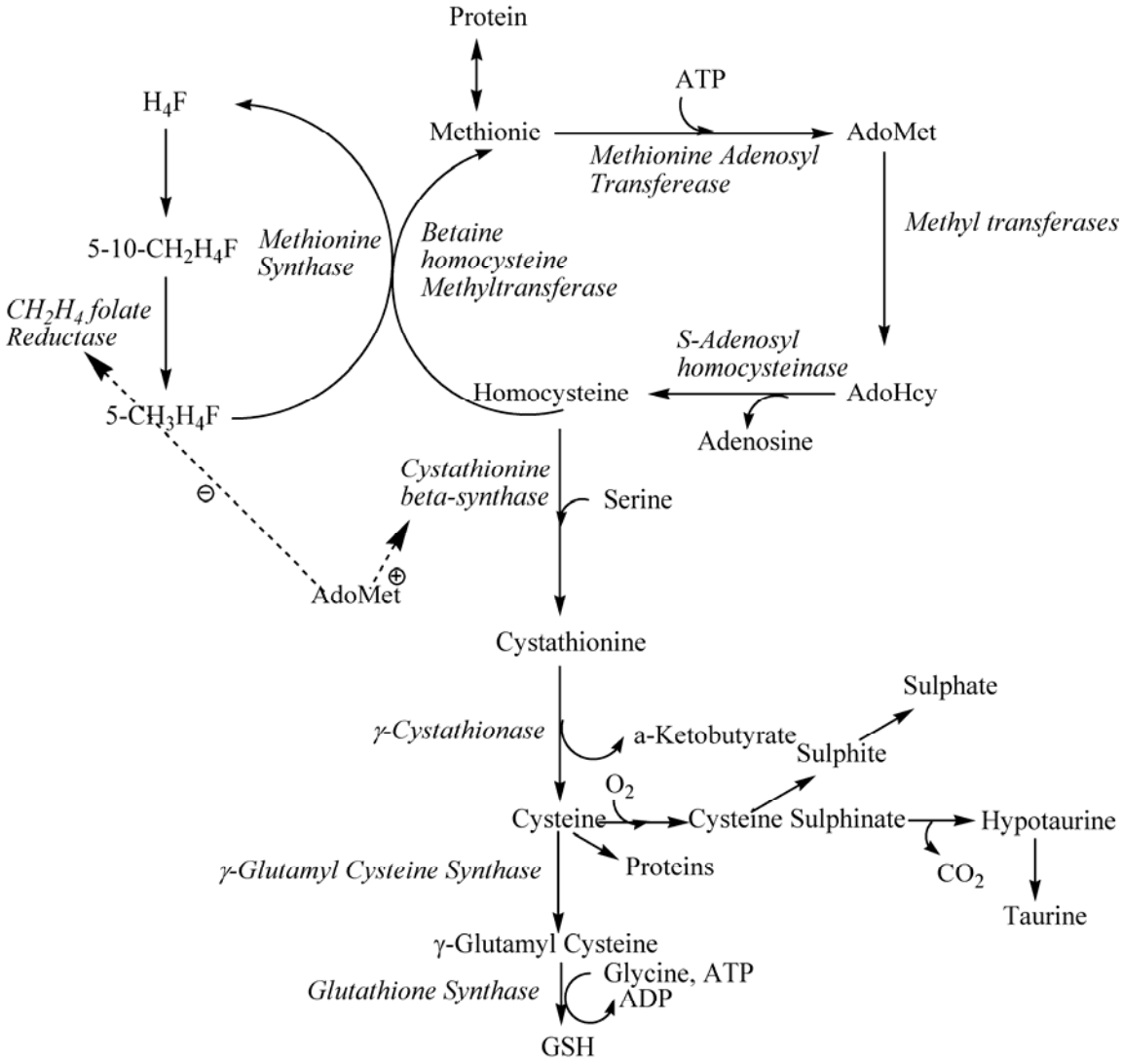

Figure1.1. An overview of homocysteine metabolism.

Enzymes involved in methionine metabolism cycle are also regulated by the redox status of the cell. AdoMet synthesis from methionine has been shown to be responsive to oxidative stress. The two isoforms of methionine adenosyltransferase that catalyze AdoMet synthesis are down-regulated under oxidative stress conditions marked by a low

GSH/GSSG ratio. This inhibition is reversed with GSH (48, 50). MS and CBS, the two enzymes which use homocysteine as a substrate, both contain redox active cofactors and are reciprocally sensitive to oxidative stress providing an additional level of regulation for switching between the methionine cycle and the transulfuration pathway (7, 56). Under oxidative conditions MS is inhibited due to the oxidation of its cofactor cob(I)calamine to cob(II)calamine and by the possible oxidative modification of the cysteine ligands to the active site zinc (7). In CBS however, redox regulation is potentially complicated and occurs at two centers in the enzyme. Studies in our laboratory have shown that the reduction of the heme in CBS leads to an approximately 2-fold diminution in its specific activity (56). On the other hand, reduction of the disulfide bridge in the CXXC motif enhances its activity (Sen S, Banerjee R, unpublished data). The opposing redox regulation by the heme and the CXXC motif of CBS activity suggests that it is most active when the CXXC motif is reduced and the heme is oxidized and least active when both redox centers are either fully reduced or fully oxidized. Addition of H_2O_2 or tertiarybutyl hydroperoxide to cultured human liver cells induces oxidative stress leading to a 2-3 fold increase in the flux of homocysteine through the transulfuration pathway (43). Another mechanism for oxidative activation of CBS is the targeted endoproteolysis to generate the truncated dimer. This is observed under some conditions, e.g. when the cytokines TNFα is added to cultured human cells (65). Under these conditions AdoMet activation is lost consistent with the cleavage of the C-terminal regulatory domain. In vitro truncated CBS has four-fold higher k_{cat} than full length CBS and is not regulated by the allosteric activator AdoMet (57). TNFα induced targeted

proteolysis of CBS is inhibited by scavengers of superoxide production or by the overexpression of manganese superoxide dismutase (65).

1.4 Impairments in homocysteine metabolism and disease

High levels of homocysteine have been correlated with various diseases affecting the cardiovascular, neural, ocular and skeletal organ systems. Mutations in CBS or in MS, the two most prevalent homocysteine-utilizing enzymes, or perturbations in their regulatory systems, lead to elevated levels of plasma homocysteine. Further mutations in homocysteine utilizing enzymes, or perturbations in their regulatory systems are the most common cause of elevated levels of plasma homocysteine. Further mutations in methyltetrahydrofolate reductase, which indirectly affects homocysteine clearance is also associated with homocystinurea as are mutations in MS reductase an enzyme required for regulation of active MS (58),(59). Elevated levels of homocysteine can also result from a diet poor in vitamins as many enzymes involved in this pathway utilizes vitamins such as folic acid, cobalamin (B_{12}) and PLP (B_6) as their cofactors. High levels of homocysteine are accompanied by high levels of AdoHcy, which is a potent inhibitor of AdoMet–dependent methylation reactions (10), (21). CBS deficiency impairs flux through the transulfuration pathway and leads to defects in sulfur metabolism including glutathione biosynthesis. In healthy individuals, plasma homocysteine levels range from 10-15 μM. Concentrations ranging from 15-100μM and > 100 μM are classified as moderate hyperhomocysteinemia and severe hyperhomocysteinemia respectively (38), (37).

Severe hyperhomocysteinemia, an inherited autosomal metabolic disorder, is characterized biochemically by high levels of homocysteine in the plasma and in the urine (39). CBS deficiency is the most common cause of hereditary hyperhomocysteinemia (45). Clinically, this disease is characterized by thrombosis, mental retardation, premature artherosclerosis, connective tissue disorders including osteoporosis, lens dislocation and skeletal abnormalities resembling Marfan syndrome with long thin extremities, decreased upper/lower segment ratio and arachnodactyly (44). Studies showed that about 30% of homocystinuric patients experience stroke or heart attack by the age of 20 (45).

Hyperhomocysteinemia due to CBS deficiency is distinct from other defects leading to homocystinurea. Connective tissue disorders are also associated with CBS deficiency (9).

1.5 CBS gene map

The CBS gene maps to the subtelomeric region of the human chromosome 21 (21q22.3) (37, 38) and contains 23 exons, spanning a region of 30 Kb. The CBS polypeptide has 551 amino acids and is encoded by exons 1 through 14 and exons 16. Exon 15 is alternatively spliced and is detected only rarely in mature mRNA molecules. The 14 amino acids encoded by this exon have not been detected in the CBS polypeptide from various mammalian tissues (33), (31). The 5' UTR of human CBS is encoded by one of five alternatively used exons, -1a b, c, d, e, and exon o present in the CBS gene. The 3'UTR is encoded by exons 16 and 17 (33). A polymorphism found in 5% of normal

Caucasian alleles has been described in which exon 8 has a 68 bp fragment insertion, 8444ins68 that is spliced out from the mature mRNA (52).

1.6 Structural and functional properties of the human CBS

Human cystathionine β-synthase (CBS), a key enzyme in sulfur metabolism, catalyzes the condensation reaction of homocysteine and serine to yield cystathionine (Scheme 1). This is the first of two PLP-dependent steps in the transulfuration pathway which converts methionine to cysteine.

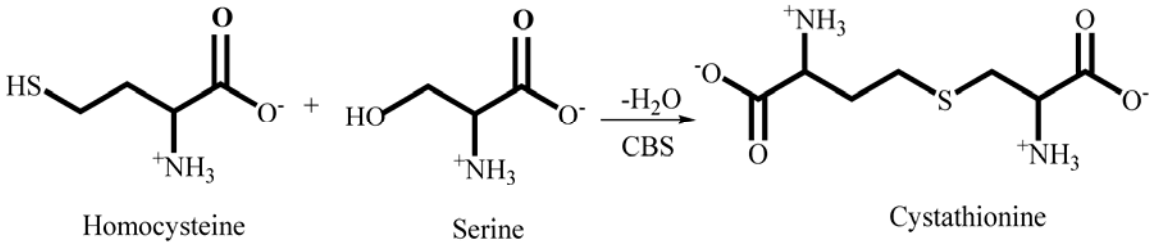

Homocysteine Serine Cystathionine

Scheme 1. Schematic representation of the reaction catalyzed by CBS.

The cysteine formed is used for multiple purposes including the synthesis of glutathione which is present at high concentrations and is involved in maintaining cellular redox balance. Under conditions of oxidative stress, the flux of sulfur through the

transulfuration pathway increases resulting in a concomitant rise in glutathione synthesis (41).

CBS is a unique PLP- dependent enzyme in that it is also heme dependent. The enzyme exists as a tetramer and a mixture of higher oligomers ranging from a dimer to a 16- mar (17). The subunit molecular weight is ~63 kDa. Each subunit binds one heme and one PLP. The V–type allosteric activator AdoMet binds stoichiometrically to each subunit and increases the activity of the enzyme by 2- to 3- fold (34).

CBS is a modular protein, the N-terminal domain of which houses the heme and PLP cofactors along with a -CPGC- motif commonly found in the active sites of thioredoxin family of proteins involved in thiol disulfide exchange reactions (22). The C-terminal domain comprises the regulatory third of the protein and houses a tandem repeat of "CBS domains", a β-α-β-β-α secondary structure motif found in a variety of unrelated proteins in all three kingdoms of life (2). AdoMet, the allosteric activator is believed to bind to the CBS domains (51).

Crystal structure of the truncated dimer of CBS

The crystal structure of a truncated dimeric form of human CBS, lacking the regulatory domain (413-551) has been solved (Fig 1.2) (24), (55). The fold of the truncated human CBS enzyme belongs to the β-family of vitamin B_6 enzymes (1) and resembles the fold found in O-acetyl-serine sulfhydrylase from *Salmonella typhimurium* (4).

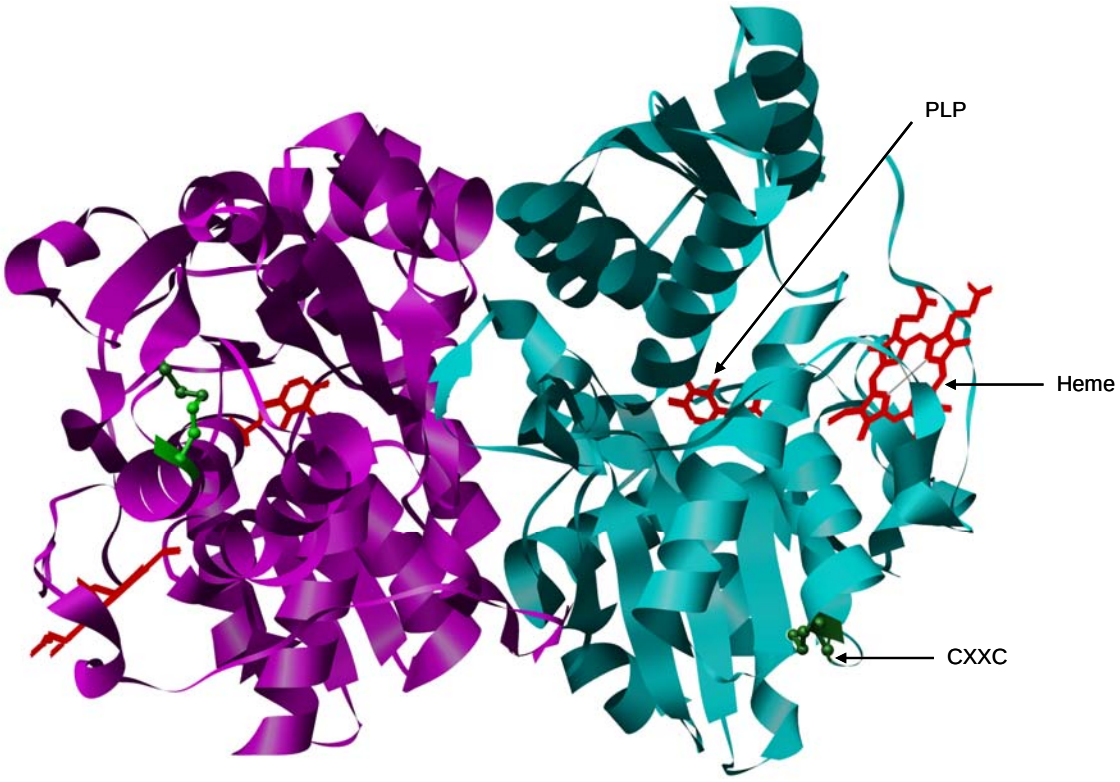

Fig 1.2. Ribbon representation of the crystal structure of the truncated dimer of CBS.

Three other PLP enzymes whose structures are known share the same fold type: tryptophan synthase (23), threonine demainase (18) and aminocyclopropane deaminase (64). A least square superposition of the C_α-positions of the structurally conserved parts between CBS and O-acetyl-serine sulfhydrylase yields a root mean square deviation of only 1.32 Å with the differences between the structures being mainly located in the loop regions.

The CBS monomer is composed of 11 α helices, seven short 3_{10} helices and two β-sheets consisting of four and six strands in the N-terminal and C-terminal domains

respectively. The heme binding domain is largely unstructured with the exception of a short 3_{10} α-helix. The dimer interface is highly hydrophobic in character. The central part of the dimer interface is formed by residues F 111 and F112 close to the 2-fold dimer axis. F 112 of one monomer thus interacts with F112 of the other. Although hydrophobic interactions dominate at the interface, polar interactions also contribute to dimer formation. PLP is deeply buried in a cleft between the N-terminal third and the C-terminal regulatory domain. The active site is accessible only by a narrow channel. The cofactor is linked to the ε-amino group of K119 via a Schiff base linkage forming the internal aldimine. The nitrogen of the pyridine ring forms a hydrogen bond to the Oγ of Ser349 similar to the other enzymes of β-family of PLP enzymes. A second hydrogen bond is formed between the 3' hydroxyl group of PLP and the $N_{\delta 2}$ of Asn149. This residue is coplanar with the pyridine ring and thus allows the expected ring tilt upon transaldimination. The phosphate binding groups Gly256, T257, G258, G259 and T260 form extended hydrogen bonds with the phosphate moiety of the PLP anchoring the cofactor to the protein matrix. Residues Y223 and G307 are probably key residues for substrate specificity, as they are spatially adjacent to the inferred substrate binding site.

The heme in CBS

Each dimer contains two hemes located at distal ends of the dimers with the orientation of their planes normal to the plane of the protein. The heme spectrum of CBS analyzed by the pyridine hemechrome method is typical of iron protophorphyrin IX (61). Ferric CBS, as isolated, exhibits a Soret absorption maximum at 428 nm and a broad αβ-band centered at ~550 nm, which is typical of low-spin 6- coordinate heme. The heme is bound in a hydrophobic pocket formed by residues 50-67, α-helices 6 and 8 and a loop

preceding β-strand 10. The sulfhydryl group of C52 and the $N_{\varepsilon 2}$ atom of H65 coordinate the heme axially. The sulfur atom of C52 is believed to be deprotonated (12) and engages in additional interactions with the side chain of R266 and the main chain nitrogen of W54. The carboxylate groups of heme are involved in ionic interactions with R51 and R224 and are partially solvent exposed unlike in cytochrome c peroxidase and cytochrome P450 iron, where the heme is buried in an internal cavity in the protein (40). Since the iron ion is ligated from both sides by protein residues and that the heme is located almost ~20 Å away from the active site, it rules out a catalytic role for heme. Carbon monoxide binds to the ferrous heme displacing the thiolate ligand (57). The enzyme retains 25% of activity under such conditions (3). Reduction of the heme from +3 to +2 oxidation state is correlated with a decrease in enzyme activity by ~1.5 fold under *in vitro* assay conditions. The Soret peak at 428 undergoes a red-shift to 450 nm under reduction of the heme with titanium citrate or dithionite (56), (46) with a concomitant sharpening of the αβ- bands at 540 and 571 respectively. A midpoint potential of -350 mV has been measured for the heme in full length CBS and -287 mV in the truncated variant (Madzelan P, Banerjee R, unpublished results). Ferric CBS shows a bell shaped pH dependence on enzyme activity with pK_{a1} and pK_{a2} values of 7.9 ± 0.2 and 8.8 ± 0.2 respectively (56). The electronic absorption spectrum of ferric CBS is independent of pH in the range 6-9 (8), indicating that a change in the heme environment is not related to the kinetic pK_as. The properties of the ferrous heme however are affected by both pH and temperature (8).

The CXXC motif in CBS

Residues 272 through 275 comprise the CXXC motif in CBS. In the crystal structure, the loop between α-helix 8 and β-strand 9 harbors this motif and is similar to that seen in active sites of disulfide oxidoreductases. The consensus sequence in this motif in oxidoreductases contains two cysteines that are linked by two residues one of which is proline (Table 1).

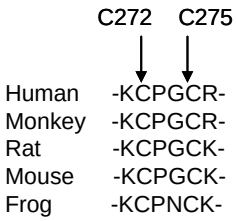

Table 1. Sequence alignment of the CXXC motif.

The CXXC motif in oxidoreductases is involved in various redox reactions in the cell, because they can be reversibly oxidized and reduced by switching between a disulfide and dithiol form during a catalytic process. In CBS, this motif consists of CPGC and forms a β turn. In the two crystal structures of truncated CBS (55), the CXXC motif is seen in both the disulfide bridge and the dithiol forms. The structure of glutaredoxin from *Escherichia coli* can be superimposed onto CBS. In this superimposition, α-helix 1 of glutaredoxin merges onto α-helix 7 of CBS, and α-helix 3 onto α-helix 8 of CBS albeit in opposite directions (55). The four strands of the central β-sheet of glutaredoxin fit onto strands 3, 8, 9 and 11 of the C-terminal domain of CBS. In CBS, the CXXC motif is

found at a location corresponding to the N-terminal end of α-helix 3 of glutaredoxin, while in glutaredoxin it is located at the N-terminal end of α-helix 1 (55). Thus, in addition to heme, the CXXC motif is another redox-active center in CBS.

1.7 Intrasteric and Allosteric Regulation in CBS

Purification of the wild-type enzyme from mammalian liver has resulted in the isolation of mixtures of the full-length as well as truncated but active dimeric forms of the enzyme (30). Limited proteolysis also yields a 45 kDa subunit and is accompanied by a change in the oligomeric state representing a dimer. This form of the enzyme represented the catalytic core and extends from amino acids 31, 37, or 40 through 413 and exhibits a k_{cat} which is 4-fold more than the full-length enzyme. The N-terminus of this polypeptide is heterogeneous due to multiple susceptible proteolytic sites at lysines 30, 36 and 39. Alternatively the catalytic-core can be generated by introduction of an opal mutation at position 409 in the open reading frame and the resulting protein extends from residues 1 to 408 (CBS-ΔC143) (54). The activity of this variant, was higher than that of the full-length (27). A truncated variant is also formed upon TNFα exposure in liver cells (65). The latter was also shown to be more active than the full-length enzyme and lacked allosteric regulation (57). Together these observations showed that the C-terminal regulatory domain imposes intrasteric regulation on the catalytic core. AdoMet which is believed to bind to the C-terminal domain of the full-length enzyme relieves this intrasteric inhibition. Binding of AdoMet increases the K_{cat} of the full length enzyme ~2

to ~3 fold, while truncation beyond the catalytic core increases k_{cat} ~4 fold compared to the basal activity associated with the full-length enzyme (57).

A patient mutation D444N located in the C-terminal domain, is highly active but is insensitive to allosteric regulation at physiological concentrations of AdoMet (11). Another interesting patient mutation P78R/K102N in the N-terminal catalytic core of the protein has recently been shown to be unresponsive to AdoMet (53). These observations suggest that there exists a significant amount of interaction between the catalytic core and the regulatory C-terminal domain. When this inter domain interaction is compromised as in the above mutants they are rendered unresponsive to AdoMet. In addition to allosteric regulation, binding of AdoMet to CBS also modulates the stability of the protein. The half life of CBS in liver cells increases from 18 to 49 h in the presence of AdoMet (49).

1.8 Mutations in CBS

Mutations in CBS are the most common cause of severe hereditary hyperhomocysteinemia (29). The vast majority of the mutations are missense with the remainder being nonsense, deletion and insertion mutations (32),(42). Characterization of patient mutations could lead to a better understanding of structural-functional correlations in CBS. Over 130 pathogenic mutations have been described that are spread over the coding and intronic sequences of the gene. The biochemical penalties associated with some of the pathogenic mutants have been addressed but the majority remains uncharacterized due to lack of a full-length crystal structure of the protein along with difficulties associated with the purification of many of the mutants which tend to form

aggregates (6), (25), (47). The two most common mutations in CBS are I278T and G307S found in an Italyan population (28). CBS mutants may or may not respond to PLP. Mutations in CBS are distributed along the whole length of the protein affecting various structural properties depending on their localization. Some such P78R, R379Q and E176K missense mutations localize to the dimer interface. Others are predicted to be at the interface between the regulatory domain and the catalytic core (62). The S466L and D444N mutations map on the CBS1 domain on the regulatory domain and the mutant proteins do not respond to the allosteric activator AdoMet as the "CBS domains" are said to be involved in nucleotide binding (62). A GST fusion of the isolated CBS domain pair (residues 416-551) from CBS was shown to bind AdoMet with a K_d of 34 μM while the D444N mutant increased the K_d by 15-fold to 510 μM (51).

References:

1. Alexander FW, Sandmeier E, Mehta PK, Christen P. 1994. Evolutionary relationships among pyridoxal-5'-phosphate-dependent enzymes. Regio-specific alpha, beta and gamma families. *Eur J Biochem* 219: 953-60
2. Bateman A. 1997. The structure of a domain common to archaebacteria and the homocystinuria disease protein. *Trends Biochem Sci* 22: 12-3
3. Bruno S, Schiaretti F, Burkhard P, Kraus JP, Janosik M, Mozzarelli A. 2001. Functional properties of the active core of human cystathionine beta-synthase crystals. *J Biol Chem* 276: 16-9

4. Burkhard P, Tai CH, Ristroph CM, Cook PF, Jansonius JN. 1999. Ligand binding induces a large conformational change in O-acetylserine sulfhydrylase from Salmonella typhimurium. *J Mol Biol* 291: 941-53

5. Carson NA, Neill DW. 1962. Metabolic abnormalities detected in a survey of mentally backward individuals in Northern Ireland. *Arch Dis Child* 37: 505-13

6. Cheesman MR, Little PJ, Berks BC. 2001. Novel heme ligation in a c-type cytochrome involved in thiosulfate oxidation: EPR and MCD of SoxAX from Rhodovulum sulfidophilum. *Biochemistry* 40: 10562-9

7. Chen Z, Chakraborty S, Banerjee R. 1995. Demonstration that mammalian methionine synthases are predominantly cobalamin-loaded. *J Biol Chem* 270: 19246-9

8. Clark RW, Youn H, Parks RB, Cherney MM, Roberts GP, Burstyn JN. 2004. Investigation of the role of the N-terminal proline, the distal heme ligand in the CO sensor CooA. *Biochemistry* 43: 14149-60

9. Dietz HC, Cutting GR, Pyeritz RE, Maslen CL, Sakai LY, et al. 1991. Marfan syndrome caused by a recurrent de novo missense mutation in the fibrillin gene. *Nature* 352: 337-9

10. Duerre JA, Wallwork JC, Quick DP, Ford KM. 1977. In vitro studies on the methylation of histones in rat brain nuclei. *J Biol Chem* 252: 6981-5

11. Evande R, Blom H, Boers GH, Banerjee R. 2002. Alleviation of intrasteric inhibition by the pathogenic activation domain mutation, D444N, in human cystathionine beta-synthase. *Biochemistry* 41: 11832-7

12. Feng L, Geck MK, Eliot AC, Kirsch JF. 2000. Aminotransferase activity and bioinformatic analysis of 1-aminocyclopropane-1-carboxylate synthase. *Biochemistry* 39: 15242-9

13. Finkelstein JD. 1998. The metabolism of homocysteine: pathways and regulation. *Eur J Pediatr* 157 Suppl 2: S40-4

14. Finkelstein JD, Kyle WE, Martin JL, Pick AM. 1975. Activation of cystathionine synthase by adenosylmethionine and adenosylethionine. *Biochem Biophys Res Commun* 66: 81-7

15. Finkelstein JD, Martin JJ. 1984. Inactivation of betaine-homocysteine methyltransferase by adenosylmethionine and adenosylethionine. *Biochem Biophys Res Commun* 118: 14-9

16. Finkelstein JD, Martin JJ. 1984. Methionine metabolism in mammals. Distribution of homocysteine between competing pathways. *J Biol Chem* 259: 9508-13

17. Frank N, Kery V, Maclean KN, Kraus JP. 2006. Solvent-accessible cysteines in human cystathionine beta-synthase: crucial role of cysteine 431 in S-adenosyl-L-methionine binding. *Biochemistry* 45: 11021-9

18. Gallagher DT, Eisenstein E, Fisher KE, Zondlo J, Chinchilla D, et al. 1998. Polymorphous crystallization and diffraction of threonine deaminase from Escherichia coli. *Acta Crystallogr D Biol Crystallogr* 54: 467-9

19. Garrow TA. 1996. Purification, kinetic properties, and cDNA cloning of mammalian betaine-homocysteine methyltransferase. *J Biol Chem* 271: 22831-8

20. Gos M, Jr., Szpecht-Potocka A. 2002. Genetic basis of neural tube defects. II. Genes correlated with folate and methionine metabolism. *J Appl Genet* 43: 511-24

21. Hoffman DR, Cornatzer WE, Duerre JA. 1979. Relationship between tissue levels of S-adenosylmethionine, S-adenylhomocysteine, and transmethylation reactions. *Can J Biochem* 57: 56-65

22. Holmgren A, Soderberg BO, Eklund H, Branden CI. 1975. Three-dimensional structure of Escherichia coli thioredoxin-S2 to 2.8 A resolution. *Proc Natl Acad Sci U S A* 72: 2305-9

23. Hyde CC, Ahmed SA, Padlan EA, Miles EW, Davies DR. 1988. Three-dimensional structure of the tryptophan synthase alpha 2 beta 2 multienzyme complex from Salmonella typhimurium. *J Biol Chem* 263: 17857-71

24. Janosik M, Meier M, Kery V, Oliveriusova J, Burkhard P, Kraus JP. 2001. Crystallization and preliminary X-ray diffraction analysis of the active core of human recombinant cystathionine beta-synthase: an enzyme involved in vascular disease. *Acta Crystallogr D Biol Crystallogr* 57: 289-91

25. Janosik M, Oliveriusova J, Janosikova B, Sokolova J, Kraus E, et al. 2001. Impaired heme binding and aggregation of mutant cystathionine beta-synthase subunits in homocystinuria. *Am J Hum Genet* 68: 1506-13

26. Kang SS, Wong PW, Malinow MR. 1992. Hyperhomocyst(e)inemia as a risk factor for occlusive vascular disease. *Annu Rev Nutr* 12: 279-98

27. Kery V, Bukovska G, Kraus JP. 1994. Transsulfuration depends on heme in addition to pyridoxal 5'-phosphate. Cystathionine beta-synthase is a heme protein. *J Biol Chem* 269: 25283-8

28. Kluijtmans LA, Boers GH, Kraus JP, van den Heuvel LP, Cruysberg JR, et al. 1999. The molecular basis of cystathionine beta-synthase deficiency in Dutch

patients with homocystinuria: effect of CBS genotype on biochemical and clinical phenotype and on response to treatment. *Am J Hum Genet* 65: 59-67

29. Kluijtmans LA, Boers GH, Trijbels FJ, van Lith-Zanders HM, van den Heuvel LP, Blom HJ. 1997. A common 844INS68 insertion variant in the cystathionine beta-synthase gene. *Biochem Mol Med* 62: 23-5
30. Kraus J, Packman S, Fowler B, Rosenberg LE. 1978. Purification and properties of cystathionine beta-synthase from human liver. Evidence for identical subunits. *J Biol Chem* 253: 6523-8
31. Kraus JP. 1998. Biochemistry and molecular genetics of cystathionine beta-synthase deficiency. *Eur J Pediatr* 157 Suppl 2: S50-3
32. Kraus JP, Janosik M, Kozich V, Mandell R, Shih V, et al. 1999. Cystathionine beta-synthase mutations in homocystinuria. *Hum Mutat* 13: 362-75
33. Kraus JP, Oliveriusova J, Sokolova J, Kraus E, Vlcek C, et al. 1998. The human cystathionine beta-synthase (CBS) gene: complete sequence, alternative splicing, and polymorphisms. *Genomics* 52: 312-24
34. Lanzilotta WN, Schuller DJ, Thorsteinsson MV, Kerby RL, Roberts GP, Poulos TL. 2000. Structure of the CO sensing transcription activator CooA. *Nat Struct Biol* 7: 876-80
35. Larkin M. 1998. Kilmer McCully: pioneer of the homocysteine theory. *Lancet* 352: 1364
36. Leboeuf R. 2003. Homocysteine and Alzheimer's disease. *J Am Diet Assoc* 103: 304-7
37. Lentz SR. 1997. Homocysteine and vascular dysfunction. *Life Sci* 61: 1205-15

38. Lentz SR, Malinow MR, Piegors DJ, Bhopatkar-Teredesai M, Faraci FM, Heistad DD. 1997. Consequences of hyperhomocyst(e)inemia on vascular function in atherosclerotic monkeys. *Arterioscler Thromb Vasc Biol* 17: 2930-4

39. McCully KS. 1969. Vascular pathology of homocysteinemia: implications for the pathogenesis of arteriosclerosis. *Am J Pathol* 56: 111-28

40. McLean KJ, Dunford AJ, Neeli R, Driscoll MD, Munro AW. 2007. Structure, function and drug targeting in Mycobacterium tuberculosis cytochrome P450 systems. *Arch Biochem Biophys*

41. Miles EW, Kraus JP. 2004. Cystathionine beta-synthase: structure, function, regulation, and location of homocystinuria-causing mutations. *J Biol Chem* 279: 29871-4

42. Moat SJ, Bao L, Fowler B, Bonham JR, Walter JH, Kraus JP. 2004. The molecular basis of cystathionine beta-synthase (CBS) deficiency in UK and US patients with homocystinuria. *Hum Mutat* 23: 206

43. Mosharov E, Cranford MR, Banerjee R. 2000. The quantitatively important relationship between homocysteine metabolism and glutathione synthesis by the transsulfuration pathway and its regulation by redox changes. *Biochemistry* 39: 13005-11

44. Mudd SH, Matorin AI, Levy HL. 1989. Homocysteine thiolactone: failure to detect in human serum or plasma. *Res Commun Chem Pathol Pharmacol* 63: 297-300

45. Mudd SH, Skovby F, Levy HL, Pettigrew KD, Wilcken B, et al. 1985. The natural history of homocystinuria due to cystathionine beta-synthase deficiency. *Am J Hum Genet* 37: 1-31

46. Ojha S, Hwang J, Kabil O, Penner-Hahn JE, Banerjee R. 2000. Characterization of the heme in human cystathionine beta-synthase by X-ray absorption and electron paramagnetic resonance spectroscopies. *Biochemistry* 39: 10542-7

47. Ojha S, Wu J, LoBrutto R, Banerjee R. 2002. Effects of heme ligand mutations including a pathogenic variant, H65R, on the properties of human cystathionine beta-synthase. *Biochemistry* 41: 4649-54

48. Pajares MA, Corrales F, Duran C, Mato JM, Alvarez L. 1992. How is rat liver S-adenosylmethionine synthetase regulated? *FEBS Lett* 309: 1-4

49. Prudova A, Bauman Z, Braun A, Vitvitsky V, Lu SC, Banerjee R. 2006. S-adenosylmethionine stabilizes cystathionine beta-synthase and modulates redox capacity. *Proc Natl Acad Sci U S A* 103: 6489-94

50. Ruiz F, Corrales FJ, Miqueo C, Mato JM. 1998. Nitric oxide inactivates rat hepatic methionine adenosyltransferase In vivo by S-nitrosylation. *Hepatology* 28: 1051-7

51. Scott JW, Hawley SA, Green KA, Anis M, Stewart G, et al. 2004. CBS domains form energy-sensing modules whose binding of adenosine ligands is disrupted by disease mutations. *J Clin Invest* 113: 274-84

52. Sebastio G, Sperandeo MP, Panico M, de Franchis R, Kraus JP, Andria G. 1995. The molecular basis of homocystinuria due to cystathionine beta-synthase deficiency in Italian families, and report of four novel mutations. *Am J Hum Genet* 56: 1324-33

53. Sen S, Banerjee R. 2007. A pathogenic linked mutation in the catalytic core of human cystathionine beta-synthase disrupts allosteric regulation and allows kinetic characterization of a full-length dimer. *Biochemistry* 46: 4110-6

54. Skovby F, Krassikoff N, Francke U. 1984. Assignment of the gene for cystathionine beta-synthase to human chromosome 21 in somatic cell hybrids. *Hum Genet* 65: 291-4

55. Taoka S, Lepore BW, Kabil O, Ojha S, Ringe D, Banerjee R. 2002. Human cystathionine beta-synthase is a heme sensor protein. Evidence that the redox sensor is heme and not the vicinal cysteines in the CXXC motif seen in the crystal structure of the truncated enzyme. *Biochemistry* 41: 10454-61

56. Taoka S, Ohja S, Shan X, Kruger WD, Banerjee R. 1998. Evidence for heme-mediated redox regulation of human cystathionine beta-synthase activity. *J Biol Chem* 273: 25179-84

57. Taoka S, Widjaja L, Banerjee R. 1999. Assignment of enzymatic functions to specific regions of the PLP-dependent heme protein cystathionine beta-synthase. *Biochemistry* 38: 13155-61

58. Toffoli G, Russo A, Innocenti F, Corona G, Tumolo S, et al. 2003. Effect of methylenetetrahydrofolate reductase 677C-->T polymorphism on toxicity and homocysteine plasma level after chronic methotrexate treatment of ovarian cancer patients. *Int J Cancer* 103: 294-9

59. Tonetti C, Ruivard M, Rieu V, Zittoun J, Giraudier S. 2002. Severe methylenetetrahydrofolate reductase deficiency revealed by a pulmonary embolism in a young adult. *Br J Haematol* 119: 397-9

60. Vanoni MA, Ballou DP, Matthews RG. 1983. Methylenetetrahydrofolate reductase. Steady state and rapid reaction studies on the NADPH-

methylenetetrahydrofolate, NADPH-menadione, and methyltetrahydrofolate-menadione oxidoreductase activities of the enzyme. *J Biol Chem* 258: 11510-4

61. Vitvitsky V, Mosharov E, Tritt M, Ataullakhanov F, Banerjee R. 2003. Redox regulation of homocysteine-dependent glutathione synthesis. *Redox Rep* 8: 57-63
62. Yamanishi M, Kabil O, Sen S, Banerjee R. 2006. Structural insights into pathogenic mutations in heme-dependent cystathionine-beta-synthase. *J Inorg Biochem* 100: 1988-95
63. Yanofsky C, Platt T, Crawford IP, Nichols BP, Christie GE, et al. 1981. The complete nucleotide sequence of the tryptophan operon of Escherichia coli. *Nucleic Acids Res* 9: 6647-68

Chapter 2

Mapping Peptides Correlated with Transmission of Intrasteric Inhibition and Allosteric Activation in Human Cystathionine β-Synthase

2.1 ABSTRACT

Cystathionine β-synthase plays a key role in the intracellular disposal of homocysteine and is the single most common locus of mutations associated with homocystinuria. Elevated levels of homocysteine are correlated with heart disease, Alzheimer's and Parkinson's diseases, and neural tube defects. Cystathionine β-synthase is modular and subjected to complex regulation, but insights into the structural basis of this regulation are lacking. We have employed hydrogen exchange mass spectrometry to map peptides whose motions are correlated with transmission of intrasteric inhibition and allosteric activation. The mass spectrometric data provide an excellent correlation between kinetically and conformationally distinguishable states of the enzyme. We also demonstrate that a pathogenic regulatory domain mutant, D444N, is conformationally locked in one of two states sampled by the wild type enzyme. Our hydrogen exchange data identify surfaces that are potentially involved in the juxtaposition of the regulatory and catalytic domains and form the basis of a docked structural model for the full-length enzyme.

2.2 Introduction

Equilibration between different conformational states often poses problems for crystallization of modular proteins, thus limiting access to structural information. Hydrogen exchange mass spectrometry is a powerful approach that can partially circumvent this limitation. Thus, motions that are correlated with interconversion between conformational states or with transduction of signals from sites distal to active

sites can be localized (*1, 2*). Human cystathionine β-synthase is an example of a modular protein that catalyzes the condensation of homocysteine and serine to give cystathionine. This represents the first step in the transsulfuration pathway that connects the methionine cycle to cysteine production and also provides an avenue for disposal of sulfur under conditions of excess (*3, 4*). The structure of a truncated catalytic core (*5, 6*) but not of the full-length protein is available, limiting structural insights into the dynamics that underlie exertion of the complex regulation associated with this enzyme. Cystathionine β-synthase is unique in being a PLP-dependent enzyme that also contains a heme b cofactor of unknown function (*7*). In this enzyme, a central catalytic core houses the active site and is interposed between an N-terminal heme domain and a C-terminal regulatory domain (Figure 1) (*3, 4*). The regulatory domain per se exerts intrasteric control over the catalytic module and its deletion results in an active form of the enzyme that displays a 4-fold higher k_{cat} but is unresponsive to the allosteric effector, *S*-adenosylmethionine (AdoMet) (*8, 9*).The regulatory domain is also important in the oligomeric architecture of the protein, and its deletion converts the native tetrameric ($\alpha4$) enzyme to a dimeric ($\alpha2$) form. This transformation from the full-length to the truncated form lacking the regulatory domain is observed in cells treated with the cytokine, TNFR, or in mice challenged with the proinflammatory agent, lipopolysaccharide (*10*). A more modest activation of the enzyme is observed with AdoMet, a V-type allosteric effector, which enhances *k*cat ~ 2-fold (*8*) and is presumed to bind to the regulatory domain (*11*).

Mutations in cystathionine β-synthase are the single most common cause of homocystinuria and over 100 disease-associated mutations have been identified in patients (*12*). A subset of these pathogenic mutations maps to the regulatory domain

appears to impose a conformational lock on the protein and is unresponsive to AdoMet (*13, 14*). While the structure of the N-terminal catalytic core of cystathionine β-synthase has been determined (*5, 6*), no structural information is available for the regulatory domain, where the allosteric activator is presumed to bind (*11*). In this study, we have employed hydrogen exchange mass spectrometry (MS) to identify peptides that respond

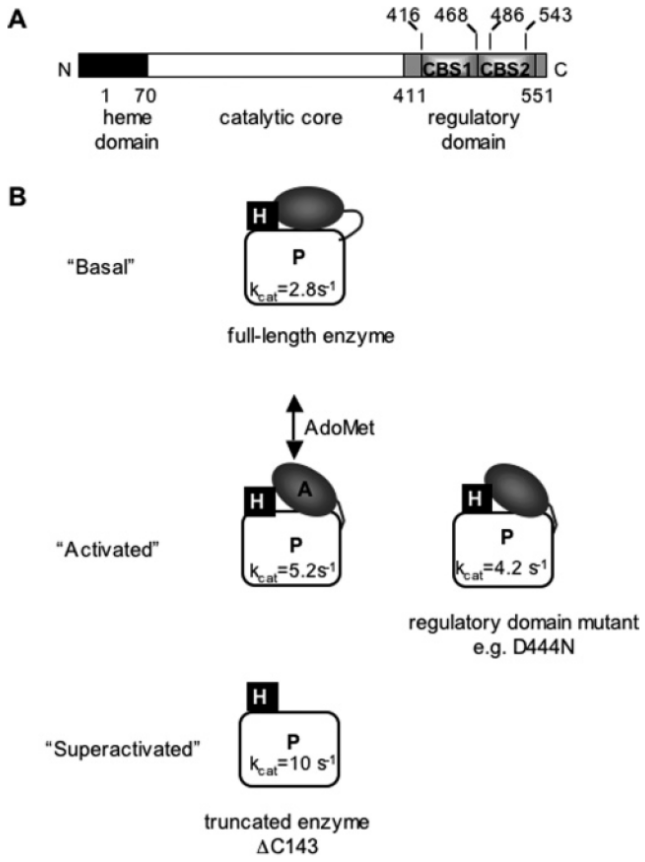

Figure 1. Modular organization and kinetic forms of human cystathionine β-synthase. A. The domains in human cystathionine β-synthase include an N-terminal heme domain, a central catalytic core and a C-terminal regulatory domain containing a tandem repeat of two CBS domains. B. Kinetically distinguishable states of human cystathionine β-synthase. A, P, and H denote AdoMet, PLP, and heme, respectively.

to the presence of AdoMet and those that respond to deletion of the regulatory domain, to locate regions associated with intrasteric inhibition and allosteric activation, respectively.

2.3 Experimental Section

Materials. Deuterium oxide (100.00 atom % D) was purchased from Sigma. Pepsin (from porcine stomach mucosa), and protease inhibitors were purchased from Sigma,porcine trypsin was from Promega and thrombin (bovine) was purchased from GenTrac Inc. Middleton, WI.

Enzyme Purification. Wild-type enzyme, the C-terminal truncated form (designated ΔC143), and the D444N mutant were expressed and purified as previously described (*8, 14, 15)*.

Limited Proteolysis of Cystathionine β-Synthase. Cystathionine β-synthase was subjected to limited proteolysis as described in the Figure 2 caption and quenched at the desired times with N^{α}-*p*-tosyl-L lysine chloromethyl ketone (Sigma).

Hydrogen-Deuterium Exchange. The feasibility of the H/D exchange MS method was initially assessed for cystathionine β-synthase by determining the sequence coverage and the spectral quality of its peptides. For this, cystathionine β-synthase (10 μg) in 100 mM ammonium phosphate buffer, pH 2.2, was centrifuged to remove any insoluble matter and digested with pepsin (1:1 w/w) for 5 min on ice. The peptic fragments were separated by HPLC and identified by tandem ESI-MS/MS as described below. Approximately 76% sequence coverage was obtained (Table 1 and Figure 2). One of the major peptides that was not observed in this analysis extends from residues 252-287 and resides in a protease

resistant core of the protein (*16*). Additionally, the peptides in the N-terminal heme domain were not detected, which could have resulted from a paucity of pepsin cleavage sites in this region. The mutant enzymes, ΔC143 and D444N (10 μg and 20 μg respectively) in 10 mM phosphate buffer, pH 6.8, were diluted 20-fold in the exchange buffer prepared in D2O (10 mM phosphate buffer, pD 6.8). For samples containing cystathionine β-synthase complexed with AdoMet, the enzyme was preincubated with 1 mM AdoMet at room temperature for 2 h. For H/D exchange studies, samples were incubated at room temperature for 5 to 60 s (to determine the effect of AdoMet) or between 5 s and 21 h (to monitor the kinetics of hydrogen exchange in full-length enzyme and the truncated variant, ΔC143) and quenched by a 2-fold dilution with 100 mM ammonium phosphate buffer, pH 2.2. The quenched samples were immediately frozen in liquid nitrogen and stored at -80 °C until further use. Following thawing, the samples were digested with pepsin as described above. To correct for loss of deuterium incurred under the experimental conditions, the peptide mass was determined using eq 1

$$D = \frac{m - m_{0\%}}{m_{100\%} - m_{0\%}} XN \qquad (1)$$

where *D* is the adjusted deuterium incorporation, *m* is the experimentally observed mass at a given time, *m*0% is the 0% or undeuterated control, *m*100% is the fully deuterated control, and *N* is the total number of exchangeable amide protons (and excludes the N-terminal proton and any proline residues). To obtain the *m*0% value, 20 μg of protein was diluted 20-fold in the quench buffer followed rapidly by the addition of an equal amount of exchange buffer in D_2O and digested with pepsin as described above. Thus, the final composition of deuterium in the quench and dilution solutions was identical for the

samples and the corresponding *m*0% control. To obtain the *m*100% value, a fully deuterated sample was prepared by incubating 20 μg of the protein overnight at room temperature in an 8 M guanidinium hydrochloride solution prepared in D_2O. The protein sample was subsequently diluted 10-fold with 100 mM ammonium phosphate, pH 2.2 (at which concentration the denaturant does not interfere with proteolytic digestion), prior to pepsin treatment. On average, ~25% of the deuterium was lost due to back exchange.

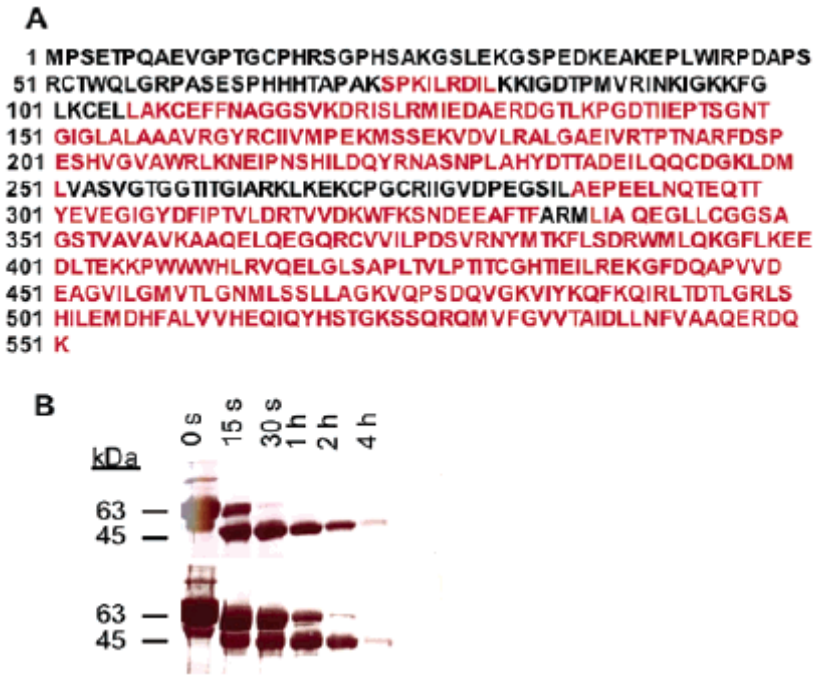

Figure 2. A. Sequence coverage of human cystathionine β-synthase obtained by MS analysis is shown in red. B. Limited proteolysis of human cystathionine β-synthase. Cystathionine β-synthase (5 nmol) was incubated at 37 °C with 750 units of porcine trypsin in 50 mM ammonium bicarbonate buffer, pH 8, in the absence (upper) or presence of 32 μM AdoMet (lower) for 0 s, 15 s, 30 s, 1 h, 2 h, and 4 h, respectively. The

reaction was quenched with 1 mM TLCK. The peptide mixture was resolved by 10% SDS PAGE and visualized by Coomassie blue staining.

Table 1. Cystathionine β-synthase peptides detected by mass spectrometry

no.	peptide boundary	sequence
1	73–81	SPKILRDIL
2	106–111	LAKCEF
3	112–124	FNAGGSVKDRISL
4	125–153	RMIEDAERDGTLKPGDTIIEPTSGNTGIG
7	127–156	IEDAERDGTLKPGDTIIEPTSGNTGIGLAL
8	154–165	LALAAAVRGYRC
9	155–165	ALAAAVRGYRC
10	166–176	IIVMPEKMSSE
11	166–181	IIVMPEKMSSEKVDVL
12	166–187	IIVMPEKMSSEKVDVLRALGAE
13	177–181	KVDVL
14	177–187	KVDVLRALGAE
15	188–197	IVRTPTNARF
16	198–222	DSPESHVGVAWRLKNEIPNSHILDQ
17	223–238	YRNASNPLAHYDTTAD
18	223–239	YRNASNPLAHYDTTADE
19	223–241	YRNASNPLAHYDTTADEIL
20	240–248	ILQQCDGKL
21	242–251	QQCDGKLDML
22	288–302	AEPEELNQTEQTTYE
23	303–315	VEGIGYDFIPTVL
24	316–323	DRTVVDKW
25	316–331	DRTVVDKWFKSNDEEA
26	316–333	DRTVVDKWFKSNDEEAFT
27	325–334	KSNDEEAFTF
28	338–355	LIAQEGLLCGGSAGSTVA
29	356–370	VAVKAAQELQEGQRC
30	371–385	VVILPDSVRNYMTKF
31	386–397	LSDRWMLQKGFL
32	386–401	LSDRWMLQKGFLKEED
33	391–397	MLQKGFL
34	398–412	KEEDLTEKKPWWWHL
35	413–426	RVQELGLSAPLTVL
36	415–426	QELGLSAPLTVL
37	417–426	LGLSAPLTVL
38	427–438	PTITCGHTIEIL
39	437–453	ILREKGFDQAPVVDEAG
40	437–457	ILREKGFDQAPVVDEAGVILG
41	437–458	ILREKGFDQAPVVDEAGVILGM
42	439–453	REKGFDQAPVVDEAG
43	439–458	REKGFDQAPVVDEAGVILGM
44	459–464	VTLGNM
45	459–468	VTLGNMLSSL
46	465–469	LSSLL
47	469–492	LAGKVQPSDQVGKVIYKQFKQIRL
48	493–510	TDTLGRLSHILEMDHFAL
49	505–510	MDHFAL
50	511–531	VVHEQIQYHSTGKSSQRQMVF
51	532–536	GVVTA
52	536–539	AIDL
53	536–541	AIDLLN
54	536–542	AIDLLNF
55	542–551	FVAAQERDQK

HPLC-ESI Mass Spectrometry. LC/ESI-MS was employed to determine the extent of deuterium incorporation into individual peptides. The HPLC injection loop, chromatographic buffers, and all the tubing used in the LC-MS set up were submerged in ice to minimize deuterium loss in this step. The peptic peptides were separated by reversed phase HPLC using a microbore C18 column (5 cm length ×1 mm internal diameter, Micro-Tech Scientific, Cousteau Court, CA). The solvents used for separation were A (water, 0.3% formic acid) and B (acetonitrile, 0.3% formic acid). The gradient was 10-35% solvent B over 20 min at a flow rate of 40μl/min. Peptides were initially identified by tandem ESI-MS/MS sequencing. The masses of individual peptides in hydrogen exchange experiments were determined by ESI MS on a Quadrupole Time-of-Flight mass spectrometer (Applied Biosystems). The peak for each peptide was integrated to obtain a centroid value using the Magtran computer program (17). The deuterium incorporation for each peptide was quantified by calculating the difference between the centroid values before and after deuterium exchange at a given time point using eq 1.

Modeled Structures. A model for the regulatory domain of human cystathionine β-synthase extending from residues 411-551 was calculated using SWISS-MODEL (*18*) using the 120 amino acid long CBS domain-containing protein from *Methanothermobacter thermautotrophicus* (Archae), strain delta H (PDB-ID 1PBJ). A docking model for the interaction between the known structure of the dimeric catalytic core (1M54) and the modeled structure of one regulatory domain was generated using ZDOCK, which combines pairwise shape complementarity with desolvation and electrostatics for scoring unbounded docking models (*19*). The search returned 3600 docking positions, with scores ranging from 62.29 to 30.09. To generate a model of the

full-length dimer, the single regulatory domain obtained from the docked model was rotated around the noncrystallographic C2 symmetry axis of the A and B chains of the catalytic domain. To narrow down the number of docked candidates, the following filter was applied: that the CR of one of the exposed residues in the 356-370 peptide in the catalytic domain (358, 359, 362, 363, 365, 366 or 369) is within 4.5-6 Å of any CR in the regulatory domain. Of the top thirty hits on the score chart, only five satisfied this criterion and the remaining models were excluded. The five candidates fell into two groups with the top two and bottom three models being very similar with respect to their overall disposition of the catalytic and regulatory domains. The bottom three models placed the regulatory domains at two ends of the dimer, making it difficult to envision them as surfaces for tetramerization. Of the two top candidates (with the 2nd and 6th highest scores in the original list of 3600 hits), one (# 6) was selected for further analysis because it afforded more favorable interactions between the dimers at the presumed dimer-dimer interface. In this model, the distance between the last structured residue in the C-terminus of the catalytic domain (CR of K395) and the first structured residue in the N-terminus of the regulatory domain (CR of Q414) is 49.1 Å, a distance that can potentially be connected by the 20 intervening amino acids.

2.4 Result and discussion

Cystathionine β-synthase is poised at a critical metabolic junction where the decision to conserve homocysteine in the methionine cycle or to commit it to transsulfuration is made. It is therefore not surprising that the enzyme is subjected to complex regulation,

which includes intrasteric inhibition imposed by the C-terminal domain and allosteric activation induced by AdoMet (*4*). Curiously, a subset of pathogenic cystathionine β-synthase mutations have been described that map to the regulatory domain, display a higher level of basal activity, but are unresponsive to AdoMet (*13*, *14*). This apparently paradoxical phenotype associated with pathogenic mutations is enigmatic and begs the question as to why they are correlated with disease. Structural insight into these regulatory modes is limited by the availability of the crystal structure of only the truncated, dimeric form of the enzyme lacking the regulatory domain. Hence, the relative juxtaposition of the regulatory and catalytic domains and the location of the dimer-dimer interface in the full-length enzyme are unknown. Kinetic studies indicate that the wild-type enzyme equilibrates between at least two conformations, the "basal" state and the "activated state", which is induced by AdoMet (Figure 1) (*14*). Limited proteolysis of wild-type cystathionine β-synthase in the presence and absence of AdoMet reveals differences in the kinetics of degradation of the protein (Figure 2), consistent with a conformational alteration. Thus, AdoMet stabilizes cleavage of the enzyme at the hypersensitive site between the catalytic and regulatory domains that converts the full-length 63 kDa subunit to a truncated 45 kDa one. The pathogenic D444N mutant exhibits a *k*cat that is similar to the "activated" state of wild-type enzyme, albeit in the absence of AdoMet, while the truncated dimer exists in a "superactivated" state, with a *k*cat that is ~4-fold higher than that of the "basal" state (Figure 1). The D444N mutation increases the *K*d for AdoMet binding to the regulatory domain from 34 ± 2 μM to 510 ± 70 μM consistent with the observed insensitivity of the mutant to physiological concentrations of the allosteric effector (*11*). Hydrogen exchange MS was employed to assess whether

these discrete kinetic states could be correlated to conformational ones and to localize peptides that are sensitive to binding of AdoMet and to deletion of the regulatory domain.

AdoMet-Induced Changes in Hydrogen Exchange Kinetics. The effect of AdoMet on the extent of deuterium incorporation was monitored over a 5 to 60 s time range. Analysis of the mass distribution profiles of > 50 peptides revealed a very focal conformational difference. The uncertainty in our mass measurements is ~ 0.2-0.3 deuteriums, and the difference in deuterium incorporation in all but one of the peptides from the two forms of the cystathionine β-synthase, fell within this range. Only a single peptide extending from residues 511-531 was identified that was sensitive to the presence of AdoMet (Figure 3B). A significant shift in the average mass from 2503.36 (-AdoMet) to 2498.24 (+AdoMet) was observed for this peptide indicative of either lower solvent accessibility or reduced hydrogen bonding in the presence of AdoMet. This represents a decrease in deuterium incorporation, from 85.5% to 51.6%, relative to the maximum deuterium incorporation possible for this peptide. The observed binomial distribution of isotope peaks for this peptide, which is characteristic of EX2 or "uncorrelated exchange" indicates that a high level of structural homogeneity exists during the deuterium exchange-in time (*20*). In other words, the unimodal distribution of the peptide mass envelope in the presence or absence of AdoMet indicates that under the present experimental conditions, the enzyme is seen to populate either the "basal" or the "activated" state and an equilibrium mixture between these two states is not detected. This is in contrast to the hematopoietic cell kinase SH3 domain in which interconverting conformers are detected by hydrogen exchange MS (*21*). Two limitations of the hydrogen exchange MS approach that are also pertinent to this study bear note. First, differences in

deuterium exchange kinetics of peptides that occur on a fast time scale (<5 s) would have been missed in this study. Second, although the 76% coverage of amino acids obtained in this experiment is relatively high, differences in the remaining 24% of the protein are missed. Approximately half of the missing residues that we were unable to detect reside in a protease resistant region of the protein, as discussed under Methods, with most of the remainder being in the N-terminal heme domain.

The D444N Mutant is Conformationally Locked in the "Activated" State. Since the pathogenic D444N mutant is unresponsive to physiological concentrations of AdoMet (*14*), the mutation could in principle have locked the protein in either the "basal" or the "activated" conformation. To distinguish between these two possibilities, the kinetics of hydrogen exchange for the D444N mutant were compared to that of wild type enzyme. They were found to be virtually identical to that of wild-type enzyme in the presence of AdoMet (Figure 3B). Thus, the D444N is locked in the "activated" conformation in the absence of AdoMet binding, which is consistent with its high basal activity and its insensitivity to physiological concentrations of AdoMet (Figure 3).

Modeled Structure of the C-Terminal Regulatory Domain. Conformational perturbation of the 511-531 peptide is particularly interesting since it is located in the C-terminal module of the enzyme (Figure 1) where AdoMet is predicted to bind (*11*). This module harbors a tandem repeat of two CBS domains, a secondary structure motif that is predicted to adopt a β-α-β-β-α fold and is found in diverse proteins in all three kingdoms of life (*22*). This domain, which derives its name from its presence in cystathionine β-synthase, is believed to function as an energy-sensing module and typically binds nucleotides (*11*). Since the structure of the full-length cystathionine β-synthase is

unavailable, we have generated a homology modeled structure of the C-terminal regulatory domain (Figure 3C) using the coordinates for a CBS domain protein from *M. thermoautotrophicus*. Pairs of CBS domains are known to dimerize to form a stable globular domain, which is also the case in the modeled structure for the cystathionine β-synthase C-terminal domain. The 511-531 peptide resides in the CBS2 domain and exhibits sensitivity to AdoMet binding and also to the D444N mutation in the CBS1 domain. The sensitivity of the 511-531 peptide could be a consequence of its proximity to the binding site for AdoMet and/or its location on the pathway of allosteric signal transduction, a distinction that cannot be made by the hydrogen exchange MS approach.

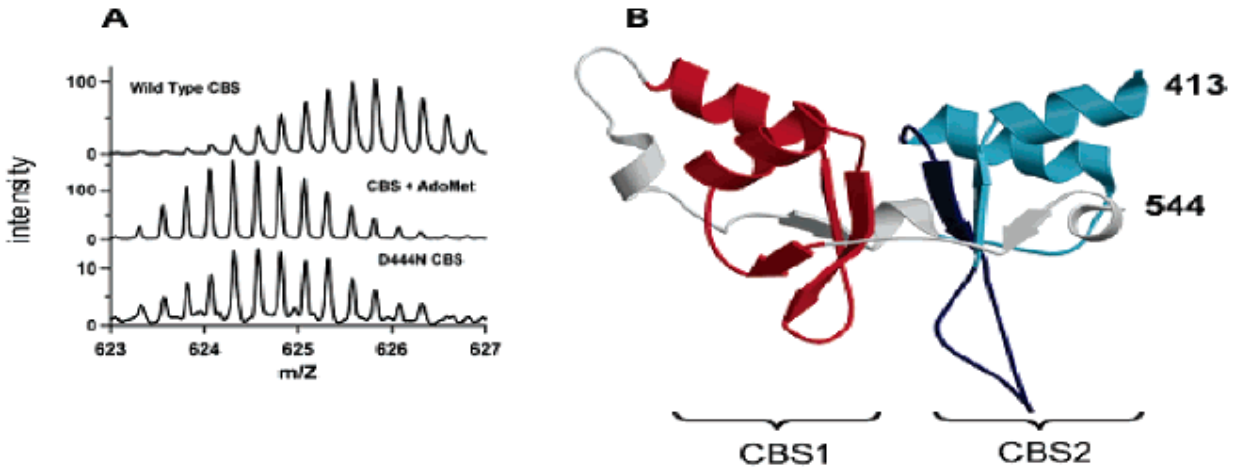

Figure 3. Mapping allosteric effects. A. Comparison of the mass analysis of the 511-531 peptide after 30 s of hydrogen exchange in wild-type enzyme without (upper) and with (middle) AdoMet and in the D444N mutant lacking AdoMet (lower). B. Location of the 513-531 peptide (in navy) in the modeled structure of the C-terminal domain. The CBS1 and CBS2 domains are shown in red and blue, respectively, and the model extends from residues 413-544 of cystathionine β-synthase.

Identification of Peptides That Respond to Deletion of the Regulatory Domain. C-Terminal truncation leads to a change in the oligomerization state from R4 to R2 and generates a "superactivated" form of the enzyme (Figure 1). This form is observed physiologically in response to a proinflamatory challenge induced by TNFR or lipopolysaccharide and increases the flux of homocysteine through cystathionine β-synthase, leading eventually to increased synthesis of the antioxidant, glutathione (*10*). Surprisingly, deletion of the regulatory domain leads to very focal changes in the kinetics of deuterium exchange within the time frame of our observations, which extended from 5 s to 21 h. Only two peptides, contiguous in sequence space, displayed significant differences in deuterium incorporation (Figure 4A-D). The first peptide extends from residues 356-370 (Figure 4E). Several amino acids in this segment are quite surface-exposed, particularly residues 358, 359, 362, 363, 365, 366, and 369. It is interesting to note that several pathogenic mutations have been reported in this stretch of cystathionine β-synthase including one, R369C/ H, which is surface exposed in the dimeric structure (*12*). A maximum difference in deuterium incorporation in this peptide was seen after a 1 min exposure to D2O (Figure 4B). The centroid mass shifted from 1635.234 (full-length) to 636.528 in the truncated enzyme, which represents a change from 25% to 41% of maximal deuterium incorporation seen for this peptide. The second peptide, extending from residues 371-385, is largely buried and resides at the interface between the monomers (Figure 4F). Only residues 382-384 in this peptide are surface-exposed and are located at the base of a cavern. A maximum mass difference in this peptide is observed after 10 min of exposure to D2O (Figure 4D). The centroid mass shifted from an average of 1788.969 (full-length) to 1791.342 (truncated), which represents an increase from 25%

to 52.1% of the maximal deuterium incorporation seen for this peptide. Several patient mutations have been identified in this stretch of cystathionine β-synthase, including one, K384N/E that is exposed in the dimeric structure (*12*).

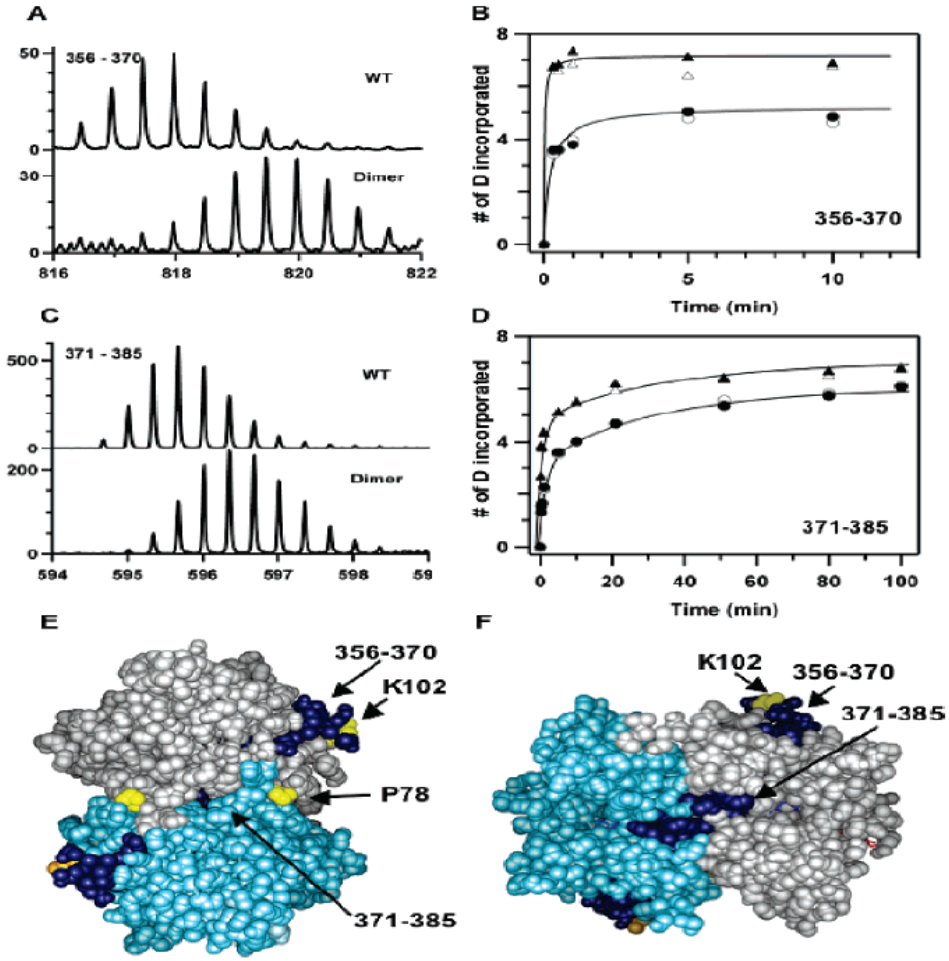

Figure 4. Mapping intrasteric effects. A. Comparison of the kinetics of hydrogen exchange of peptides 356-370 (A) and 371-385 (B) that respond to deletion of the regulatory domain. The spectra in A and B represent samples that were quenched after 1 min. C and D show the differences in the kinetics of deuterium incorporation in the 356-370 peptide in the truncated (circles) and full-length (triangles) protein (C) and for the 371-385 peptide in truncated (circles) and full length (triangles) protein (D). The closed

and open symbols represent data from two independent experiments. E. Location of the 356-370 and 371-385 peptides (in navy) in the crystal structure of the catalytic core shown in surface representation. The subunits are shown in gray and blue, and the residues, P78 and K102, that are mutated in some homocystinuric patients and lead to lack of AdoMet sensitivity are shown in yellow. F. A different view of the truncated dimer highlighting the location of the 371-385 peptide.

A Modeled Structure for Full-Length Cystathionine β*-Synthase.* The hydrogen exchange data identifies two surfaces in the dimeric structure that experience greater solvent accessibility or reduced hydrogen bonding interactions upon deletion of the regulatory domain (Figure 4E and 4F). We have employed the MS data in conjunction with the reported properties of cystathionine β-synthase to guide our selection of a model for the full-length enzyme (Figure 5) generated by the ZDOCK program. It is important, however, to first note some limitations of this model-building exercise. In principle, it is possible that the peptides identified in this study report indirectly on the loss of the regulatory domain with a consequent change in the oligomeric organization, and that the actual interaction surfaces were missed due to the time course of the kinetic analysis. Hydrogen exchange rates for individual amides in a protein can vary over several orders of magnitude (*23*), and only those amides with half-lives for exchange that are similar to the experimental labeling time report on structural changes (*20*). Thus, a limitation of this study is that hydrogen exchange kinetics were monitored in a time range from seconds to

hours, and differences in dynamics and/or structure that resulted in differences in deuterium incorporation rates on a shorter time scale would have been missed. We propose that both the 356-370 and the 371-385 peptides are likely to be reporting on deletion of the regulatory domain based on the following lines of reasoning. Cystathionine β-synthase exists as a homotetramer that separates into dimers following a proteolytic clip between the catalytic and regulatory domains (*16*). Thus, interactions between the regulatory domains appear to be more important in preserving the tetrameric structure than interactions between the catalytic domains. We propose that the 356- 370 peptide is involved in making direct contact with the regulatory domain based on its proximity to the P78 and K102 residues (Figure 4E). Mutations in these two residues (P78R/K102N) are inherited as linked pathogenic mutations in homocystinurics (*12*). The P78R/K102N mutations impair sensitivity to AdoMet, suggesting their proximity to the regulatory domain (Sen and Banerjee, manuscript in preparation). The docked model generated by ZDOCK provides an excellent fit to our assignment of this region as the regulatory-catalytic domain interface (Figure 5 A). The exposed surface of the 371-385 peptide is located at the bottom of a cavity (Figure 5A) and leads to a short helix that ends in a loop representing the C-terminus of the catalytic domain. In the intact structure, this loop would lead to the regulatory domain and its truncation could perturb the environment of the 371-385 peptide, resulting in changes in the kinetics of deuterium incorporation. The location and the limited surface exposure of this largely buried peptide appear to be incompatible with its possible involvement in the dimer-dimer interface (Figure 5). Based on the docked model of the dimer, we propose a schematic model for the organization of the full-length enzyme (Figure 5B). In this model, the regulatory

domains on adjacent monomers are on opposite edges of the dimer and contact the mirror domains in the tetramer. This model is consistent with the known properties of the wild type and mutant enzymes, the role of the regulatory domain in tetramerization, and with the separation of dimers following deletion of this domain. In this model, the regulatory domains form the dimer-dimer interface and generation of the truncated dimer exposes on the catalytic domain only those surfaces that are sensitive to loss of the regulatory domain. This is consistent with our ascription of the sensitivity of both the 356-370 and 371-385 peptides to deletion of the regulatory domain. The validity of this model will of course be tested as additional insights into cystathionine β-synthase are gained and ultimately by the crystal structure of the full-length enzyme itself.

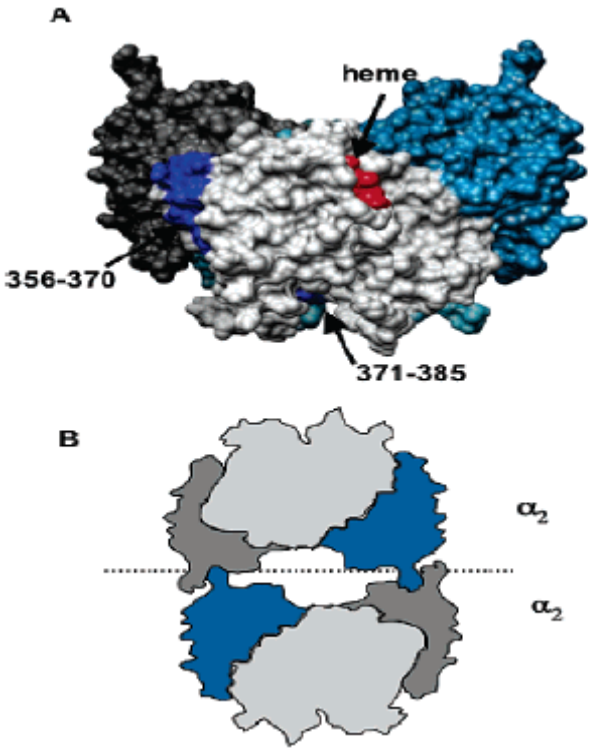

Figure 5. Modeled structure of full-length cystathionine β-synthase. A. A docked model showing the predicted juxtaposition of the regulatory domains and the catalytic core of

the dimer. The two catalytic domains are shown in light gray and light blue, respectively, while the corresponding regulatory domains are shown in darker shades. The light blue subunit is behind the plane of the light gray subunit and not visible. A portion of the 356-370 peptide (in navy) on one of the chains and of the heme (in red) are visible in this view. This model was generated using ZDOCK as described under Methods. B. Model of the full-length cystathionine β-synthase showing the relative juxtaposition of two R2 dimers. The color scheme used in A is retained.

2.5 Conclusions

In summary, we have localized focal conformational changes in wild-type cystathionine β-synthase that are induced by AdoMet, to a peptide which spans residues 511- 531 in the regulatory domain. Furthermore, we have demonstrated that this "activated" conformation is mimicked by the pathogenic D444N mutation, explaining its known insensitivity to AdoMet (*14, 24*). This approach could be useful for providing structural insights into other pathogenic mutants. The kinetics of hydrogen exchange reveal two surfaces that are sensitive to deletion of the regulatory domain. This information has been used to build a structural model of the full-length human enzyme (Figure 5), which could be helpful in providing a framework for understanding the interactions between the regulatory and catalytic modules and the penalties associated with pathogenic mutants.

2.6 Acknowledgement

The authors thank David Smith (University of Nebraska, Lincoln) for his helpful comments on the manuscript. The Mass Spectrometry Core Facility of the Redox Biology Center (University of Nebraska, Lincoln) was used in this study and supported by a grant from the NIH (P20RR17675).

References

1. Hoofnagle, A. N., Resing, K. A., and Ahn, N. G. (2003) Protein analysis by hydrogen exchange mass spectrometry, *Annu. Re*V. *Biophys. Biomol. Struct 32*, 1-25.
2. Engen, J. R., and Smith, D. L. (2000) Investigating the higher order structure of proteins. Hydrogen exchange, proteolytic fragmentation, and mass spectrometry, *Methods Mol. Biol*. *146*, 95-112.
3. Miles, E. W., and Kraus, J. P. (2004) Cystathionine {beta}- Synthase: Structure, Function, Regulation, and Location of Homocystinuria-causing Mutations, *J. Biol. Chem*. *279*, 29871- 29874.
4. Banerjee, R., and Zou, C. G. (2005) Redox regulation and reaction mechanism of human cystathionine-beta-synthase: a PLP-dependent hemesensor protein, *Arch. Biochem. Biophys*. *433*, 144- 56.
5. Meier, M., Janosik, M., Kery, V., Kraus, J. P., and Burkhard, P. (2001) Structure of human cystathionine beta-synthase: a unique pyridoxal 5′- phosphate-dependent heme protein, *EMBO J*. *20*, 3910-6.

6. Taoka, S., Lepore, B. W., Kabil, O., Ojha, S., Ringe, D., and Banerjee, R. (2002) Human cystathionine beta-synthase is a heme sensor protein. Evidence that the redox sensor is heme and not the vicinal cysteines in the CXXC motif seen in the crystal structure of the truncated enzyme, *Biochemistry 41*, 10454-61.

7. Kery, V., Bukovska, G., and Kraus, J. P. (1994) Transsulfuration depends on heme in addition to pyridoxal 5-phosphate. Cystathionine β-synthase is a heme protein, *J. Biol. Chem. 269*, 25283-25288.

8. Taoka, S., Widjaja, L., and Banerjee, R. (1999) Assignment of enzymatic functions to specific regions of the PLP-dependent hemeprotein cystathionine *â*-synthase, *Biochemistry 38*, 13155- 13161.

9. Shan, X., and Kruger, W. D. (1998) Correction of disease causing CBS mutations in yeast, *Nature Genet. 19*, 91-93.

10. Zou, C.-G., and Banerjee, R. (2003) Tumor necrosis factor-α induced targeted proteolysis of cystathionine beta-synthase modulates redox homeostasis, *J. Biol. Chem. 278*, 16802-16808.

11. Scott, J. W., Hawley, S. A., Green, K. A., Anis, M., Stewart, G., Scullion, G. A., Norman, D. G., and Hardie, D. G. (2004) CBS domains form energy-sensing modules whose binding of adenosineligands is disrupted by disease mutations, *J. Clin. In*V*est. 113*,274-84

12. Kraus, J. P., Janosik, M., Kozich, V., Mandell, R., Shih, V.,Sperandeo, M. P., Sebastio, G., deFranchis, R., Andria, G., Kluijtmans, L. A., Blom, H., Boers, G. H., Gordon, R. B., Kamoun, P., Tsai, M. Y., Kruger, W. D., Koch, H. G., Ohura, T.,

and Gaustadnes, M. (1999) Cystathionine beta-synthase mutations in homocystinuria, *Hum. Mutat. 13*, 362-75.

13. Janosik, M., Kery, V., Gaustadnes, M., Maclean, K. N., and Kraus, J. P. (2001) Regulation of human cystathionine beta-synthase by S-adenosyl-L- methionine: evidence for two catalytically active conformations involving an autoinhibitory domain in the Cterminal region, *Biochemistry 40*, 10625-33.
14. Evande, R., Boers, G. H. J., Blom, H. J., and Banerjee, R. (2002) Alleviation of Intrasteric Inhibition by the Pathogenic Activation Domain Mutation, D444N, in Human Cystathionine beta-synthase, *Biochemistry 41*, 11832-11837.
15. Taoka, S., Ohja, S., Shan, X., Kruger, W. D., and Banerjee, R. (1998) Evidence for heme-mediated redox regulation of human cystathionine β-synthase activity, *J. Biol. Chem. 273*, 25179- 25184.
16. Kery, V., Poneleit, L., and Kraus, J. (1998) Trypsin cleavage of human cystathionine beta-synthase into an evolutionarily conserved active core: Structural and functional consequences, *Arch. Biochem. Biophys. 355*, 222-232.
17. Zhang, Z., and Smith, D. L. (1993) Determination of amide hydrogen exchange by mass spectrometry: a new tool for protein structure elucidation, *Protein Sci. 2*, 522-31.
18. Schwede, T., Kopp, J., Guex, N., and Peitsch, M. C. (2003) SWISS-MODEL: An automated protein homology-modeling server, *Nucleic Acids Res. 31*, 3381-5.
19. Chen, R., Li, L., and Weng, Z. (2003) ZDOCK: an initial-stage protein-docking algorithm, *Proteins 52*, 80-7.

20. Smith, D. L. (1998) Local structure and dynamics in proteins characterized by hydrogen exchange and mass spectrometry, *Biochemistry (Mosc) 63*, 285-93.

21. Engen, J. R., Smithgall, T. E., Gmeiner, W. H., and Smith, D. L. (1997) Identification and localization of slow, natural, cooperative unfolding in the hematopoietic cell kinase SH3 domain by amide hydrogen exchange and mass spectrometry, *Biochemistry 36*, 14384-91.

22. Bateman, A. (1997) The structure of a domain common to archaebacteria and the homocystinuria disease protein., *Trends Biochem. Sci. 22*, 12-13.

23. Englander, S. W., Downer, N. W., and Teitelbaum, H. (1972) Hydrogen exchange, *Annu. Re*V. *Biochem. 41*, 903-24.

24. Kluitjmans., L. A. J., Boers., G. H. J., Stevens., E. M. B., Renie., W. O., Kraus., J. P., Trijbels., F. J. M., Heuvel., L. P. W. J. v. d., and Blom., H. J. (1996) Defective cystathionine beta-synthase regulation by S-adenosylmethionine in a partially pyridoxine responsive homocystinuria, *J. Clin. In*V*est. 98*, 285-289.

Chapter 3

A pathogenic Linked Mutation in the Catalytic Core of Human Cystathionine β-Synthase Disrupts Allosteric Regulation and Allows Kinetic Characterization of a Full-Length Dimer

3.1 Abstract

Cystathionine β-synthase catalyzes the condensation of serine and homocysteine to yield cystathionine and is the single most common locus of mutations associated with homocystinuria. In this study, we have examined the kinetic consequences of a pair of linked patient mutations, P78R/K102N, that are housed in the catalytic core of the protein and compared it to the effects of the corresponding single mutations. The P78R mutation affords purification of a mixture of higher order oligomers, P78R-I, which resembles the mixed quaternary state associated with wild type enzyme. However, unlike wild type enzyme, P78R-I converts over time to P78R-II, which exists predominantly, as a full-length dimer. The specific activities of the K102N, P78R-I and P78R-II mutants in the absence of AdoMet are ~3-, 9- and 3-fold lower than of wild-type enzyme and are stimulated 2.9-, 2.5- and 1.4-fold respectively by AdoMet. However, when linked, the specific activity of the resulting double mutant is comparable to that of wild-type enzyme but it is unresponsive to AdoMet, revealing that interactions between the two sites modulate the phenotype of the enzyme. Steady-state kinetic analysis for the double mutant reveals a sigmoidal dependence on homocysteine that is not observed with wild-type enzyme, which is ascribed to the mutation at the K102 locus and indicates changes in subunit interactions. Hydrogen-deuterium mass spectrometric analyses reveals that even in the absence of AdoMet, the double mutant is locked in an activated conformation that is observed for wild-type enzyme in the presence of AdoMet, providing a structural rationale for loss of this allosteric regulation. To our knowledge, this is the first example of mutations in the catalytic core of cystathionine b-synthase that result in failure of AdoMet-dependent regulation. Furthermore, analysis of individual single mutations has

permitted for the first time, partial kinetic characterization of a full-length dimeric form of human cystathionine β-synthase.

3.2 Introduction

Cystathionine β-synthase is a pyridoxal phosphate (PLP)[1]-dependent protein that catalyzes the condensation of serine and homocysteine to give cystathionine and is activated by the allosteric effector, AdoMet (*1-3*). It catalyzes the first step in the transsulfuration pathway connecting the methionine cycle to cysteine production. Mutations in cystathionine β-synthase are the single most common cause of hereditary hyperhomocysteinemia and over one hundred pathogenic mutations have been described so far (*4*). They represent a roadmap of residues that are important for the structural and/or functional integrity of the enzyme and characterization of these mutants have begun to provide invaluable insights into the organization and regulation of this unusual enzyme (*5-9*). The pathogenic mutations are dispersed over all three domains of the modular protein: the N-terminal heme domain, which is found in some but not all eukaryotic cystathionine β-synthases, the central active site domain where PLP is bound and the C-terminal regulatory domain, which is required for allosteric activation of the enzyme by AdoMet.

The purified human enzyme is a homooligomer with a subunit mass of 63 kDa and exists in multiple higher order oligomeric states ranging from a dimer to a 16-mer (*10*), which have not been purified and characterized separately to date (Figure 1). A hypersensitive site leads to the facile proteolytic separation between the catalytic core and

the regulatory domain (*11*). The resulting truncated enzyme is a well-behaved dimer that is not prone to aggregation unlike the full-length enzyme. It has a subunit mass of 45 kDa and exhibits an ~4-fold higher k_{cat} than the full-length form (*9*) but is unresponsive to AdoMet (*12*). The regulatory domain thus appears to be autoinhibitory and its cleavage alleviates inhibition of cystathionine β-synthase activity (*11-13*). Furthermore, truncation is accompanied by a change in the oligomerization state of the protein from tetramer to dimer. These results reveal a complex role for the C-terminal domain in mediating regulation of cystathionine β-synthase including intrasteric and allosteric regulation and in the oligomerization of the protein beyond the dimeric state.

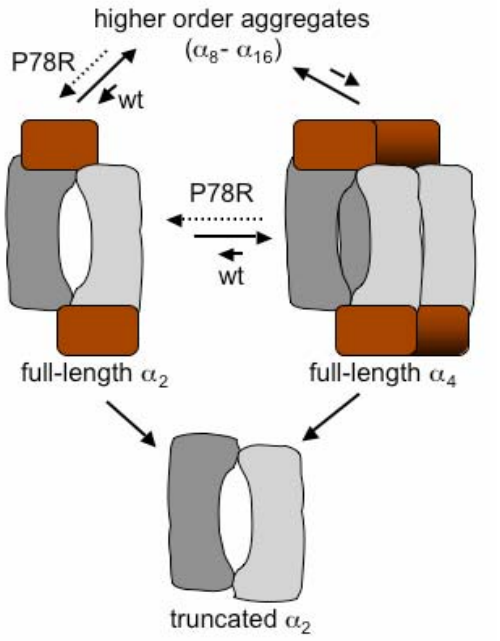

Figure 1. Model of the oligomeric heterogeneity seen with human cystathionine β-synthase. It is not known whether the equilibrium between the different oligomeric states

involves dissociation into monomers and has been shown for simplicity, to involve either the dimer or the tetramer. The P78R mutation shifts the equilibrium towards the full-length dimer compared to wild type enzyme. Deletion of the regulatory domain leads to a truncated dimer.

A class of pathogenic mutations housed in the regulatory domain has been described that display a common and seemingly paradoxical phenotype (*6, 9, 14, 15*). When mimicked in vitro, these regulatory domain mutants are unresponsive to activation by AdoMet but exhibit robust enzyme activity comparable to or greater than that of wild type enzyme (*6, 9*). Mathematical modeling of methionine metabolism provides a rationale for the build up of homocysteine by the mere loss of allosteric activation of cystathionine β-synthase, particularly under conditions of methionine excess, confirming an important role for AdoMet-dependent regulation in intracellular homocysteine homeostasis (16).

The crystal structure of the catalytic core of cystathionine β-synthase has been reported and reveals the relative juxtaposition of the heme- and PLP-domains (*17, 18*). However, the structure of the regulatory domain and its interaction with the catalytic core are unknown. The C-terminal domain is comprised of a tandem repeat of two CBS domains, a β-α-β-β-α secondary structure motif that is found in diverse proteins in all three kingdoms of life and believed to function as an energy sensor (*19, 20*). A homology-modeled structure of the catalytic core has been generated based on the crystal structure of a CBS-domain containing protein from *Methanobacter thermoautotrophicus*

(21). The only structural insights that are presently available on the mechanism of allosteric signal transduction between the regulatory and the catalytic domain derives from hydrogen exchange MS studies, which identified a single peptide in the CBS2 domain extending from residues 511-531 that exhibits a lower propensity for deuterium incorporation in the presence of AdoMet (21). In combination with other hydrogen exchange MS data, these studies have been used to build a docked model of the regulatory and catalytic domains (Figure 2) (21), which in the absence of a crystal structure for the full-length enzyme, provides a useful framework for interpreting the functional data (*22*). Although the regulatory domain is believed to house the binding site for AdoMet (20), the role of the CBS domains in cystathionine β-synthase, the protein from which this motif derives its name, is unknown.

In this study, we report on the characterization of a linked patient nucleotide mutation, C233G/G306C, corresponding to P78R/K102N in the polypeptide, which are located in the catalytic core of the protein (Figure 2). These paternally inherited cis mutations have been described in three siblings who, like most homocystinurics, are compound heterozygotes, and have a maternally inherited E239K mutation in the other allele (*23*). Interestingly, the siblings display a wide range of clinical phenotypes from severe (in the two sisters) to benign (in the brother) despite sharing an identical genotype at this locus, which indicates possible gender-dependent modulation of the expression of cystathionine β-synthase-dependent homocystinuria. Previous studies of the P78R/K102N mutation were limited to cell lysates of *Escherichia coli* expressing recombinant cystathionine β-synthase (*23*). We have analyzed, using purified recombinant human cystathionine β-synthase, the biochemical penalties associated with

the individual mutations to elucidate the contribution of each locus to the phenotype of the double mutant. The P78R mutation allowed for the first time, limited kinetic characterization of a full-length dimeric form of cystathionine β-synthase. Interestingly, interactions between the K102N and P78R mutations result in a compound phenotype that is similar to but also distinct from those of the single mutants. The double mutant is as active as the wild-type enzyme but is unresponsive to the allosteric activator, AdoMet. The loss of allosteric regulation is explained by hydrogen exchange MS data, which revealed that the linked mutation locks the protein in a conformation achieved by wild-type enzyme in the presence of AdoMet. To our knowledge, this is the first example of mutations in the catalytic core that confer AdoMet insensitivity, exhibit high basal activity and thus resemble a subset of regulatory domain mutations that have been described in homocystinuric patients.

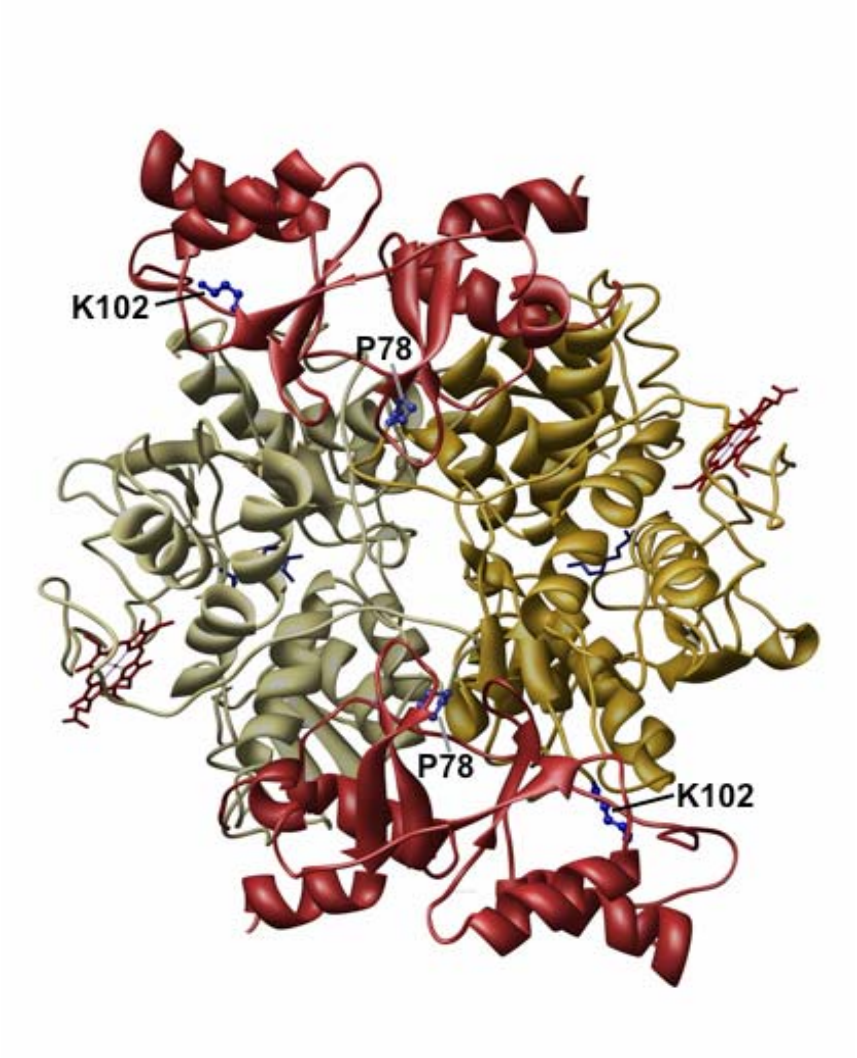

Figure 2. Modeled structure of full-length cystathionine β-synthase dimer showing locations of the P78 and K102 residues. The structure was generated by docking the crystal structure of the catalytic core of cystathionine β-synthase (in tan) with the homology modeled structure of the regulatory domain (in scarlet) as described previously (21). The locations of P78 and K102 (in blue ball and stick representation) are indicated as are of the heme (in red) and PLP (in blue).

3.3 Material and methods

Materials-Serine, IPTG, and D, L-homocysteine were purchased from Sigma. [^{14}C]-Serine (158 mCi/mmol) was purchased from Amersham. GST Sepharose and Superdex$_{TM}$ 200 were purchased from Pharmacia. Deuterium oxide (100.00 atom % D) was purchased from Sigma. AdoMet 1,4-butanedisulfonate was a generous gift from Knoll Farmaceutici Spa (Milano, Italy). Thrombin was purchased from GenTrac Inc. Middleton, WI. Complete tablets (protease cocktail inhibitors) were purchased from Roche Diagnostics (Mannheim, Germany).

Generation of the CBS Mutants and Protein Purification-The single mutants K102N, P78R and the double mutant P78R/K102N, were generated by site-directed mutagenesis using the Quick Change Kit from Stratagene. The template for mutagenesis was pGEX4T1/hCBS containing wild-type human cystathionine β-synthase gene fused in-frame with glutathione *S*-transferase (*24*). The forward and the reverse primers that were employed were:

P78R: Sense: 5' :CCAAAATCTTGCGAGATATTCT

Antisense: 5': AGAATATCTCGCAAGATTTTTGG

K102N: Sense: 5': AAGTTCGGCCTGAACTGTGAGCTCTTGGC

Antisense: 5': GCCAAGAGCTCACAGTTCAGGCCGAACTT

The double mutant, P78R/K102N, was constructed by introducing the P78R mutation using the single mutant, K102N as template, and the appropriate set of primers. The mutations were confirmed by nucleotide sequencing at the Genomics Core Facility at the University of Nebraska Lincoln.

Protein purification and enzyme assays- The mutant enzymes were expressed in *E. coli* and purified as glutathione *S*-transferase fusion proteins using recombinant expression systems essentially as described for wild-type enzyme (*24*). The cell extract was prepared and sonicated in 50 mM Tris HCl pH 8, supplemented with protease inhibitor cocktail tablets (Roche Diagnostics). One tablet was used for the 300 ml cell extract prepared from a 6 l culture.

Following partial proteolysis by thrombin (1 U/mg protein) to remove the GST tag, the K102N and P78R/K102N mutants were dialyzed to remove glutathione and purified by anion exchange chromatography as described previously (*24*). The P78R mutant was purified following thrombin digestion by gel filtration chromatography using a 90 X 3 cm Superdex TM 200 column eluted isocratically with 50 mM Tris HCl containing 0.1 M NaCl. Over 50 mg of ~90% pure protein was obtained from 6 l of culture for each mutant.

The enzyme activity was assayed under aerobic conditions using 30 mM [^{14}C]-serine and 30 mM D,L-homocysteine as described previously (*13*). One unit of enzyme activity catalyzes the conversion of 1 μmol cystathionine min^{-1} at 37˚C. Protein concentration was determined by the Bradford method using bovine serum albumin as a standard. The concentration of the stock homocysteine solution was determined immediately prior to the experiments by titration with 5,5'-dithiobis 2-nitrobenzoic acid and estimated using a value of ε_{412} of 13,600 M^{-1} cm^{-1}.

Steady-state kinetic analysis was performed in the standard radiolabeled assay and initiated by addition of homocysteine. The reaction mixture was incubated for 30 min at 37˚C and terminated by the addition of 200 μl of 10% trifluoroacetic acid. The

radiolabeled product, [^{14}C]-labeled cystathionine, was separated from [^{14}C]-labeled serine as described previously (*13*). The kinetic sbehavior of some mutants (indicated in Table I) showed a sigmoidal rather than a hyperbolic dependence on substrate concentration and these data were fitted to the Hill equation to obtain the Hill coefficient.

Hydrogen-deuterium exchange mass spectrometry- These experiments were performed with wild type and the P78R/K102N forms of cystathionine β-synthase exactly as described previously (21). To correct for loss of deuterium incurred under the experimental conditions, the peptide mass was determined using equation 1 where D is the adjusted deuterium incorporation, m is the experimentally observed mass at a given time, $m_{0\%}$ is the 0 percent or undeuterated

$$D = \frac{(m - m_{0\%})}{(m_{100\% - m0\%})} XN \qquad \text{Equation 1}$$

control, $m_{100\%}$ is the fully deuterated control and N is the total number of exchangeable amide protons (and excludes the N-terminal proton and any proline residues). To obtain the $m_{0\%}$ value, 20 µg of protein was diluted 20-fold in the quench buffer followed rapidly by the addition of an equal amount of exchange buffer in D_2O and digested with pepsin as described above. Thus, the final composition of deuterium in the quench and dilution solutions was identical for the samples and the corresponding $m_{0\%}$ control.

To obtain the $m_{100\%}$ value, a fully deuterated sample was prepared by incubating 20 µg of the protein overnight at room temperature in an 8 M guanidinium hydrochloride solution prepared in D_2O. The protein sample was subsequently diluted 10-fold with 100 mM ammonium phosphate, pH 2.2 (at which concentration the denaturant does not interfere with proteolytic digestion), prior to pepsin treatment.

HPLC-ESI Mass Spectrometry- LC/ESI-MS was employed to determine the extent of deuterium incorporation into individual peptides as described previously (21). The masses of individual peptides in hydrogen exchange experiments were determined by ESI-MS on a Quadrupole time-of-flight mass spectrometer (Applied Biosystems). The peak for each peptide was integrated to obtain a centroid value using the Magtran computer program (*25*). The deuterium incorporation for each peptide was quantified by calculating the difference between the centroid values before and after deuterium exchange at a given time point using equation 1.

Native gel electrophoresis for determining oligomeric state- Protein samples (30 μg each) were separated on a 4-20% gradient gel under nondenaturing conditions. The gels were run at 4˚C at 120 V and 15 mA current.

3.4 Results

Purification and Oligomeric States of the K102N, P78R and P78R/K102N Mutants- The recombinant single and double mutants were obtained in at least 90% purity as determined by electrophoresis under denaturing conditions and by the ratio of the 280 nm to 428 nm absorption peak (which is ~1 for pure wild type enzyme (*24*)). The PLP content of both the single and the double mutants was identical to that of wild type enzyme, i.e. one PLP per subunit (data not shown). The P78R single mutant exhibited a shift in the equilibrium distribution of oligomeric states that was detected by analysis of freshly purified enzyme. Gel filtration chromatography resulted in elution of P78R as a broad peak and partial resolution of two species designated hereafter as P78R-I and

P78R-II respectively, as revealed by native gel electrophoresis (Figure 3). P78R-I migrated as a mixture of higher-order oligomers, which is also observed with wild-type enzyme, whereas P78R-II is predominantly in the dimeric state. Storage of P78R-I at 4˚C for 24-48 h resulted in its conversion to the P78R-II state. In contrast, the K102N and the double mutant behaved like wild-type enzyme by native gel chromatography and exists as a mixture of higher-order quaternary states.

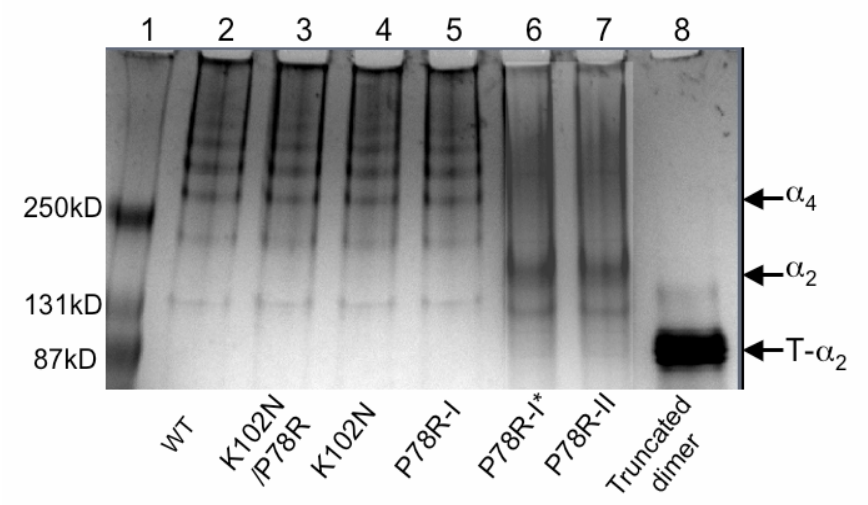

Figure 3. The P78R-II mutant behaves like a dimer. Native gel electrophoresis of wild type cystathionine β-synthase and various single and double mutants shows heterogenous oligomeric states. P78R-I* refers to the form obtained by overnight incubation of P78R-I at 4˚C. Lane 1 shows migration of molecular weight markers and lane 8, the truncated dimeric form of cystathionine β-synthase (T-α_2) which has a molecular mass of ~90 kDa.

Kinetic Properties of the K102N, P78R and P78R/K102N Mutants- The steady-state kinetic parameters for the variants were compared with those of wild type enzyme (Table

1). Each of the single mutants diminished the specific activity with the K102N showing a 3-fold lower activity (65 μmol mg^{-1} h^{-1}) and the P78R-I and P78R-II forms exhibiting 9- (19 μmol mg^{-1} h^{-1}) and 3-fold (62 μmol mg^{-1} h^{-1}) lower activity than wild type enzyme (178 μmol mg^{-1} h^{-1}). Overnight storage of P78R-I at 4°C resulted in its conversion to P78R-II and was accompanied by a 3-fold increase in specific activity to 58 ± 5 μmol mg^{-1} h^{-1}. Interestingly, the deficits in activity associated with each of the single mutations were negated in the double mutant (169 μmol mg^{-1} h^{-1}), which was as active as wild-type enzyme in the absence of AdoMet.

Some changes were observed in the kinetic parameters for the substrates. The K_M for serine is ~2-fold higher for the K102N and P78R/K102N mutants and ~4-fold higher for the P78R-II mutant compared to wild-type enzyme. A sigmoidal dependence of activity on serine concentration was seen with P78R-I with a Hill coefficient of 2.4. Sigmoidal kinetics are observed with the K102N single and the P78R/K102N double mutants when homocysteine is the variable substrate with a Hill coefficient of 3, indicating positive cooperativity. The K_M for L-homocysteine is 2-fold higher for the K102N mutant, lower for the P78R-II mutant, and comparable to wild-type enzyme for the double mutant (Table I).

Table 1. Comparison of kinetic parameters of the single and double mutants with wild-type cystathionine β-synthase

Enzyme	Wild type	P78R-I	P78R-II	K102N	K102N/P78R
S.A.[a](+AdoMet)	378 ± 17	47 ± 4	84 ± 2	185 ± 4	169 ± 9
k_{cat}[b] (+AdoMet)	6.6 sec^{-1}	0.8sec^{-1}	1.4 sec^{-1}	3.0 sec^{-1}	3.0 sec^{-1}
S.A. (-AdoMet)	178 ± 5	19 ± 2	62 ± 0.5	65 ± 9	169 ± 9
k_{cat} (-AdoMet)	3.0 sec^{-1}	0.3 sec^{-1}	1.0 sec^{-1}	1.0 sec^{-1}	3.0 sec^{-1}
K_{MSer} (mM)	2.0 ± 0.3	1.9 ± 0.2	8 ± 3	3.8 ± 0.8	5.1 ± 0.8
Hill Coefficient[c]	-	2.4 ± 0.7	-	-	-
K_{MHcy} (mM)	5.0 ± 0.9	5 ± 2	2.4 ± 0.5	10 ±1	4.4 ± 0.3
Hill Coefficient	-	-	-	3 ±1	3.0 ± 0.2

[a] Specific activity is in units of μmol cystathionine formed h^{-1} mg^{-1} protein.

[b] k_{cat} is calculated based on the molecular mass of the monomer. Hill coefficients are reported only when a sigmoidal dependence on substrate concentration was observed. In all other instances, the K_M values were obtained by Michaelis-Menten analysis of the data set.

The P78R/K102N Mutant is Insensitive to Allosteric Regulation. In the presence of AdoMet, the specific activity of wild-type cystathionine β-synthase increases ~2-fold from 178 μmol mg^{-1} h^{-1} to 378 μmol mg^{-1} h^{-1} (*24*). The K102N and P78R-I variants exhibit sensitivity to AdoMet and were activated 2.9- and 2.5-fold respectively. In

contrast, P78R-II, which exists predominantly in the dimeric state, shows diminished activation (1.4-fold) by AdoMet. Based on the densitometric analysis of the native gel, we estimate that ~30% of P78R-II is present in the higher oligomeric state. Thus, the AdoMet responsiveness of P78R-II indicates that the full-length dimer is also sensitive to allosteric regulation. In contrast, the P78R/K102N double mutant is unresponsive to AdoMet. Thus, interaction between the P78 and K102 positions in the double mutant results in loss of allosteric regulation.

Hydrogen Exchange MS Reveals Conformational Lock in the P78R/K102N Mutant. Hydrogen exchange MS was employed to determine if the insensitivity of the double mutant results from a conformational lock in the kinetically distinguishable "basal" and "activated" states (Figure 4A). Of the ~50 peptides that were identified for the double mutant, a significant difference in the extent of deuterium incorporation was observed in only one peptide, extending from residues 511-531 (Figure 4B) with a mass of 2502.704. The same peptide in wild-type enzyme had previously been shown to exhibit a downshift in the centroid mass from 2503.36 in the absence to 2498.24 in the presence of AdoMet (21). This corresponds to a decrease in maximal deuterium incorporation from 85% in the wild-type enzyme to 51% in the double mutant. The P78R/K102N double mutant thus appears to be conformationally locked in the "activated" state, explaining its insensitivity to AdoMet. The decrease in deuterium concentration upon exposure to AdoMet in wild-type enzyme and in the double mutant as isolated, indicates decreased solvent exposure and/or hydrogen bonding interaction in this conformation.

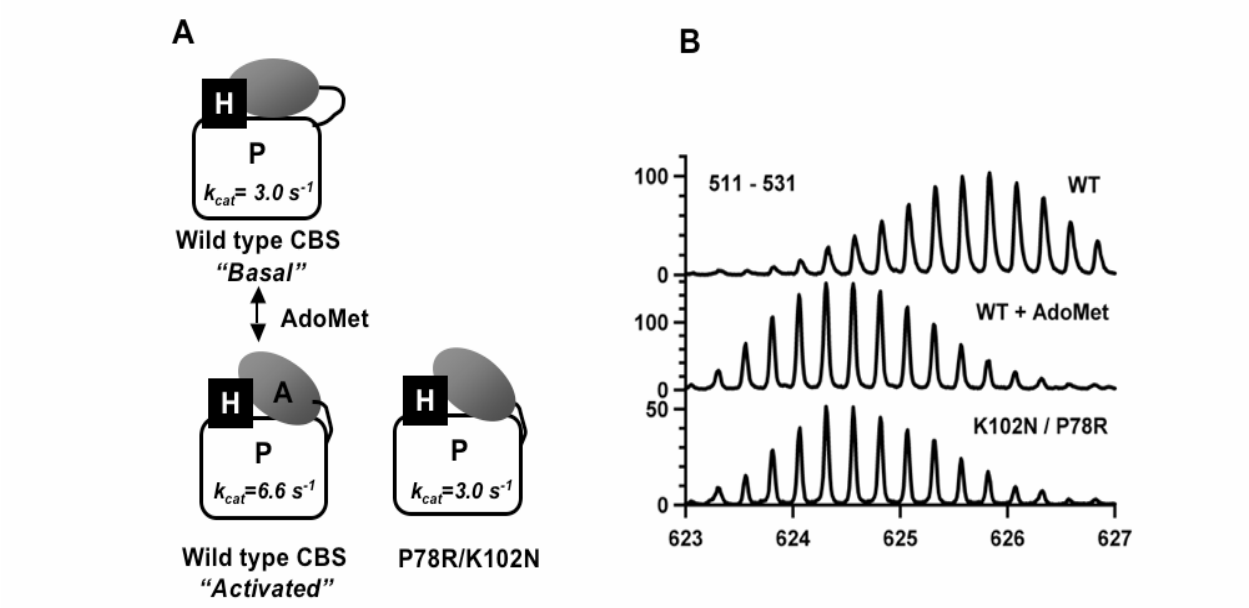

Figure 4. Conformational change induced by AdoMet binding to cystathionine β-synthase. A. Model of an AdoMet-induced conformational change in cystathionine β-synthase. The model correlates differences in kinetic properties associated with the basal and activated states of cystathionine β-synthase with the structural changes revealed by hydrogen-deuterium mass spectrometry. The P78R/K102 patient mutation is locked in the activated conformation even in the absence of AdoMet. B. Mass spectrometric analysis of wild-type and the P78R/K102N mutants of cystathionine β-synthase. Hydrogen-deuterium exchange mass spectrometric analysis of cystathionine β-synthase identified a single peptide extending from residues 511 to 531 that revealed a difference in the centroid mass after 30 s of hydrogen exchange in the presence (m/z = 624.803) versus absence (m/z = 625.676) of AdoMet. The same peptide in the double mutant in the *absence* of AdoMet, exhibited a centroid mass corresponding to that observed with wild-type enzyme in the *presence* of AdoMet.

Discussion

Pathogenic mutations represent Nature's map of residues that are important for the structural and/or functional integrity of proteins. In the case of cystathionine β-synthase, over 100 patient mutations have been described that are dispersed across all three domains of the modular protein (*4*). Biochemical characterizations of a limited number of missense mutations that are remote from the active site have been described (*5-9*) and have provided novel insights into clinically important phenotypes associated with specific mutations, viz. pyridoxine responsiveness. A subset of pathogenic mutations, clustered in the CBS1 domain of the regulatory module are associated with an interesting phenotype, i.e. they show robust basal activity but are unresponsive to allosteric activation by AdoMet (*6, 9, 14*). Biophysical characterization of one such mutant, D444N, revealed that it is conformationally locked in an activated state that is observed with wild-type enzyme only in the presence of AdoMet (21). These studies reveal that AdoMet binding to the regulatory domain shifts the conformation of cystathionine β-synthase from a kinetically distinguishable "basal" state to an "activated" state, which in turn, increases the activity of the enzyme. In this study, we have examined the penalties associated with a pair of linked mutations P78R/K102N, described in homocystinuric patients and compared them to the deficits associated with the single mutations.

Wild-type human cystathionine β-synthase exists as a mixture of oligomeric states with higher-order oligomers being the predominant species. Analysis of wild-type cystathionine β-synthase by blue native gel electrophoresis reveals the presence of oligomers ranging from a dimer to ~16-mers (*10*). However, the kinetic properties associated with the full-length dimer have not been reported because of the difficulty in

separating the various oligomeric states in pure form. P78 is located at the periphery of the dimer interface in the crystal structure of truncated cystathionine β-synthase (*22, 26*) (Figure 2). Unlike wild-type enzyme, chromatography of P78R results in partial separation of two oligomeric states monitored by native gel chromatography, which correspond to a predominantly full-length dimeric form (P78R-II) and a mixture of higher oligomeric forms (P78R-I). The P78R-I form is unstable and is converted to the P78R-II state over 24 h at 4˚C, permitting limited kinetic characterization of the full-length dimeric form of cystathionine β-synthase (Table 1). The principal findings for P78R-II, which is enriched in the full-length dimer, is that it is active, albeit ~3-fold less so than wild-type enzyme, and is responsive to allosteric activation by AdoMet. The K_M values for both serine and homocysteine for P78R-II are similar to those for wild-type enzyme. The P78R-I form, which is a heterogeneous mixture of oligomeric states is 3-fold less active than P78R-II and exhibits K_M values for the two substrates that are similar to wild-type enzyme. Extrapolating from these results to wild-type enzyme, suggests that a dimeric form of cystathionine β-synthase would be active and AdoMet responsive. The physiological relevance of the oligomeric heterogeneity associated with purified human cystathionine β-synthase is not known, nor what ligands or metabolic state might favor one versus other structures. Since the full-length dimer of P78R is associated with higher activity compared to the mixed higher-order oligomeric state, P78R-I, it raises the possibility that stabilization of the full-length dimer may be used as a mechanism for upregulation of wild-type cystathionine β-synthase under certain conditions.

The instability of the P78R-I form together with the absence of the homogenous dimeric form in the P78R-II pool, limited our ability to further characterize their

oligomeric states by biophysical methods viz. analytical ultracentrifugation, which yielded variable results. It also raises questions about whether the kinetic properties of the P78R-II species that we have determined, truly reflect those for the full-length dimer. In fact, we estimate that ~30% of the P78R-II pool represents higher-order oligomers. Unfortunately, we have been unable to purify the dimeric form any further using various chromatographic columns. Nonetheless, the observed differences in the kinetic properties between P78R-I and -II, particularly with respect to specific activity, lends confidence at least to the qualitative differences between the dimer and the mixed higher oligomeric states that are reported in this study.

The principal in vitro biochemical phenotypes associated with the linked patient mutation, P78R/K102N, are high basal activity comparable to wild-type enzyme and AdoMet unresponsiveness. The high basal activity exhibited by the P78R/K102N enzyme indicates that the mutant retains a full complement of PLP. This is curious in light of the B_6-responsive phenotype associated with patients carrying this mutation (*23*). It is possible that the B_6-responsiveness is associated with the second mutation in these patients, E239K. We also note the seeming paradox between pyridoxine responsiveness in patients carrying the I278T mutation in cystathionine β-synthase, which is not reflected in an altered affinity for PLP in the expressed protein (27). This observation led the authors of the study to suggest that the clinical response to pyridoxine may involve multiple mechanisms (27).

Since neither single mutant exhibits this property, we conclude that their interaction in the double mutant is responsible for this phenotype. The insensitivity of the double mutant to AdoMet could arise in principle from its inability to bind the allosteric activator

and therefore be locked in the "basal" conformation or to it being locked in the "activated" conformation that is seen with wild-type enzyme in the presence of AdoMet (Figure 4A). The AdoMet responsive peptide identified by hydrogen exchange MS reveals that in the catalytic domain mutations, P78R/K102N, as in the regulatory mutation, D444N, the exchange kinetics for this peptide in the *absence* of AdoMet mimic that for wild type enzyme, in the *presence* of AdoMet (Figure 4B). Thus, the double mutant exhibits an identical conformational signature in a regulatory domain peptide that is seen with wild type enzyme in the presence of AdoMet or the regulatory domain mutant, D444N (Figure 4). To our knowledge, this is the first demonstration of mutations in the catalytic core that mimic the AdoMet insensitivity of a subclass of CBS1-domain mutations (*6, 9*).

The K102N mutation exhibits only mild deficits being ~2- to 3-fold less active than wild type enzyme in the absence or presence of AdoMet (Table 1). The distinguishing kinetic feature of this mutant is that it exhibits non-Michaelis Menten kinetics when homocysteine is the variable substrate and the sigmoidal dependence is associated with a Hill coefficient of 3. This feature is also observed in the double mutant, which exhibits a K_M for homocysteine that is comparable in value to that of wild-type enzyme but exhibits positive cooperativity with a Hill coefficient of 3. Thus, the change in interaction between subunits in the double mutant with respect to homocysteine binding can be ascribed to the missense mutation at the K102 locus. Interestingly, the individual single mutants are each less active than the double mutant indicating favorable compensatory changes in the linked pair that restores basal activity to wild-type levels.

An earlier study had reported preliminary characterization of the single and double mutants in *E. coli* cell extracts (*23*). Both the P78R and K102N single mutants exhibited fairly variable activity that were 2- to 10-fold lower than wild type enzyme, depending on the clone. The authors reported seeing no activity with the double mutant. These results are inconsistent with those reported in this study for the P78R/K102N mutant and also with the absence of a classical homocystinuric clinical phenotype in one of the siblings in whom this mutation has been described, especially since the other mutation in this patient, E239K, has also been reported by the same group to be associated with no activity in cell extracts (*23*). The basis of the discrepancy between the two studies is not known. However, it is interesting to note that other patients with nonclassical homocystinuria have been described who also have mutations that map to the regulatory domain of cystathionine β-synthase and result in AdoMet-unresponsiveness (15). These patients exhibit high plasma homocysteine levels in the absence of the neurological or connective tissue defects classically associated with homocystinuria due to cystathionine β-synthase deficiency. This clinical presentation is reminiscent of the male patient with the AdoMet-unresponsive P78R/K102N double mutation, associated with nonclassical homocystinuria (*23*).

Computational studies have revealed that insensitivity to allosteric activation by AdoMet can result in hyperhomocysteinemia particularly under conditions of high methionine intake when the transsulfuration pathway becomes especially important in disposing off excess methionine and homocysteine (*16*). While the AdoMet-unresponsiveness of the P78R/K102N mutation could similarly predispose patients to hyperhomocysteinemia, the interaction with subunits containing the second mutation

found in these patients, E239K, may significantly alter the phenotype of the encoded protein. Alternatively, the nucleotide changes associated with the double mutation could alter gene expression.

Finally, although known for some time in laboratories that work on this protein, the oligomeric heterogeneity associated with wild-type cystathionine β-synthase has not been characterized primarily due to the difficulty in stably resolving the different enzyme forms. The P78R mutation appears to afford some stabilization of the dimer, which has permitted the limited characterization reported in this study. It is not known if some or all of the multiple oligomeric states of cystathionine β-synthase are constructed from monomers (or dimers) that have slightly different conformations, and therefore qualify as "morpheeins", a model for allostery in which the monomer conformation dictates the resulting oligomeric state (28). The analysis of an uncommon allele of human porphobilinogen synthase allowed isolation and crystallization of a hexameric form, distinct from the octamer seen with wild-type enzyme and led to the morpheein concept (29). Elegant studies have since shown that it is the quaternary structure change rather than the amino acid change that underlies the differences in the kinetic properties of the two variants of porphobilinogen synthase (*29, 30*). We currently have insufficient data to evaluate whether or not a dynamic morpheein equilibrium is responsible for the multiple quaternary states of cystathionine β-synthase but note that some of the kinetic attributes of morpheeins viz. dependence of activity on order of substrate addition and hysteresis, have been observed with cystathionine β-synthase (*13*).

Acknowledgements

We thank Dr. Jiong Yu in the Mass Spectrometry Center of the Redox Biology Center (University of Nebraska, Lincoln) for help with data accumulation.

References

1. Banerjee, R., Evande, R., Kabil, O., Ojha, S., and Taoka, S. (2003) Reaction mechanism and regulation of cystathionine beta-synthase. *Biochim Biophys Acta 1647*, 30-5.
2. Banerjee, R., and Zou, C. G. (2005) Redox regulation and reaction mechanism of human cystathionine-beta-synthase: a PLP-dependent hemesensor protein. *Arch Biochem Biophys 433*, 144-56.
3. Miles, E. W., and Kraus, J. P. (2004) Cystathionine {beta}-Synthase: Structure, Function, Regulation, and Location of Homocystinuria-causing Mutations. *J Biol Chem 279*, 29871-29874.
4. Kraus, J. P., Janosik, M., Kozich, V., Mandell, R., Shih, V., Sperandeo, M. P., Sebastio, G., de Franchis, R., Andria, G., Kluijtmans, L. A., Blom, H., Boers, G. H., Gordon, R. B., Kamoun, P., Tsai, M. Y., Kruger, W. D., Koch, H. G., Ohura, T., and Gaustadnes, M. (1999) Cystathionine beta-synthase mutations in homocystinuria. *Hum Mutat 13*, 362-75.

5. Kabil, O., and Banerjee, R. (1999) Deletion of the regulatory domain in the pyridoxal phosphate-dependent heme protein cystathionine beta-synthase alleviates the defect observed in a catalytic site mutant. *J Biol Chem 274*, 31256-60.

6. Janosik, M., Kery, V., Gaustadnes, M., Maclean, K. N., and Kraus, J. P. (2001) Regulation of human cystathionine beta-synthase by S-adenosyl-L- methionine: evidence for two catalytically active conformations involving an autoinhibitory domain in the C-terminal region. *Biochemistry 40*, 10625-33.

7. Janosik, M., Oliveriusova, J., Janosikova, B., Sokolova, J., Kraus, E., Kraus, J. P., and Kozich, V. (2001) Impaired heme binding and aggregation of mutant cystathionine beta- synthase subunits in homocystinuria. *Am J Hum Genet 68*, 1506-13.

8. Ojha, S., Wu, J., LoBrutto, R., and Banerjee, R. (2002) Effects of heme ligand mutations including a pathogenic variant, H65R, on the properties of human cystathionine beta syntase. *Biochemistry 41*, 4649-4654.

9. Evande, R., Boers, G. H. J., Blom, H. J., and Banerjee, R. (2002) Alleviation of Intrasteric Inhibition by the Pathogenic Activation Domain Mutation, D444N, in Human Cystathionine beta-synthase. *Biochemistry 41*, 11832 - 11837.

10. Frank, N., Kery, V., Maclean, K. N., and Kraus, J. P. (2006) Solvent-accessible cysteines in human cystathionine beta-synthase:Crucial role of cysteine 431 in S-adenosyl L-methionine binding. *Biochemistry 45*, 11021-11029.

11. Kery, V., Poneleit, L., and Kraus, J. (1998) Trypsin cleavage of human cystathionine beta-synthase into an evolutionarily conserved active core: Structural and functional consequences. *Arch. Biochem. Biophys. 355*, 222-232.

12. Shan, X., and Kruger, W. D. (1998) Correction of disease causing CBS mutations in yeast. *Nature Genetics 19*, 91-93.

13. Taoka, S., Widjaja, L., and Banerjee, R. (1999) Assignment of enzymatic functions to specific regions of the PLP-dependent hemeprotein cystathionine b-synthase. *Biochemistry 38*, 13155-13161.

14. Kluitjmans., L. A. J., Boers., G. H. J., Stevens., E. M. B., Renie., W. O., Kraus., J. P., Trijbels., F. J. M., Heuvel., L. P. W. J. v. d., and Blom., H. J. (1996) Defective cystathionine beta-synthase regulation by S-adenosylmethionine in a partially pyridoxine responsive homocystinuria. *J. Clin. Invest. 98*, 285-289.

15. Maclean, K. N., Gaustadnes, M., Oliveriusova, J., Janosik, M., Kraus, E., Kozich, V., Kery, V., Skovby, F., Rudiger, N., Ingerslev, J., Stabler, S. P., Allen, R. H., and Kraus, J. P. (2002) High homocysteine and thrombosis without connective tissue disorders are associated with a novel class of cystathionine beta-synthase (CBS) mutations. *Hum Mutat 19*, 641-55.

16. Prudova, A., Martinov, M. V., Vitvitsky, V., Ataullakhanov, F., and Banerjee, R. (2005) Analysis of pathological defects in methionine metabolism using a simple mathematical model. *Biochim Biophys Acta 1741*, 331-8.

17. Meier, M., Janosik, M., Kery, V., Kraus, J. P., and Burkhard, P. (2001) Structure of human cystathionine beta-synthase: a unique pyridoxal 5'- phosphate-dependent heme protein. *EMBO J 20*, 3910-6.

18. Taoka, S., Lepore, B. W., Kabil, Ö., Ojha, S., Ringe, D., and Banerjee, R. (2002) Human cystathionine beta-synthase is a heme sensor protein. Evidence that the

redox sensor is heme and not the vicinal cysteines in the CXXC motif seen in the crystal structure of the truncated enzyme. *Biochemistry 41*, 10454-61.

19. Bateman, A. (1997) The structure of a domain common to archaebacteria and the homocystinuria disease protein. *Trends Biochem. Sci. 22*, 12-13.
20. Scott, J. W., Hawley, S. A., Green, K. A., Anis, M., Stewart, G., Scullion, G. A., Norman, D. G., and Hardie, D. G. (2004) CBS domains form energy-sensing modules whose binding of adenosine ligands is disrupted by disease mutations. *J Clin Invest 113*, 274-84.
21. Sen, S., Yu, J., Yamanishi, M., Schellhorn, D., and Banerjee, R. (2005) Mapping Peptides Correlated with Transmission of Intrasteric Inhibition and Allosteric Activation in Human Cystathionine beta-Synthase. *Biochemistry 44*, 14210-6.
22. Yamanishi, M., Kabil, Ö., Sen, S., and Banerjee, R. (2006) Structural Insights into Pathogenic Mutations in Heme-dependent Cystathionine-β-synthase. *J. Inorg. Bioc.*, accepted for publication.
23. de Franchis, R., Kozich, V., McInnes, R. R., and Kraus, J. P. (1994) Identical genotypes in siblings with different homocystinuric phenotypes: identification of three mutations in cystathionine beta-synthase using an improved bacterial expression system. *Hum Mol Genet 3*, 1103-8.
24. Taoka, S., Ohja, S., Shan, X., Kruger, W. D., and Banerjee, R. (1998) Evidence for heme-mediated redox regulation of human cystathionine b-synthase activity. *J. Biol. Chem. 273*, 25179-25184.

25. Zhang, Z., and Smith, D. L. (1993) Determination of amide hydrogen exchange by mass spectrometry: a new tool for protein structure elucidation. *Protein Sci 2*, 522-31.

26. Meier, M., Oliveriusova, J., Kraus, J. P., and Burkhard, P. (2003) Structural insights into mutations of cystathionine beta-synthase. *Biochim Biophys Acta 1647*, 206-13.

27. Chen, X., Wang, L., Fazlieva, R., and Kruger, W. D. (2006) Contrasting behaviors of mutant cystathionine beta-synthase enzymes associated with pyridoxine response. *Hum Mutat 27*, 474-82.

28. Jaffe, E. K. (2005) Morpheeins--a new structural paradigm for allosteric regulation. *Trends Biochem Sci 30*, 490-7.

29. Breinig, S., Kervinen, J., Stith, L., Wasson, A. S., Fairman, R., Wlodawer, A., Zdanov, A., and Jaffe, E. K. (2003) Control of tetrapyrrole biosynthesis by alternate quaternary forms of porphobilinogen synthase. *Nat Struct Biol 10*, 757-63.

30. Tang, L., Stith, L., and Jaffe, E. K. (2005) Substrate-induced interconversion of protein quaternary structure isoforms. *J Biol Chem 280*, 15786-93.

Chapter 4

Redox Potentials of the Heme and CXXC Motif and their Modulation of Human Cystathionine β-synthase Activity

4.1 Abstract

Cystathionine β-synthase (CBS) is a heme containing PLP-dependent enzyme that condenses serine and homocysteine to form cystathionine. CBS is the first enzyme in the transsulfuration pathway, commits homocysteine to cysteine synthesis, and is subject to complex regulation. In addition to heme, human CBS has a second putative redox-active center, a CXXC motif comprising the residues C272-P273-G274-C275, whose role in regulating enzyme activity is not known. In this study, we have developed a new assay for CBS that uses a non-thiol substrate analog, homoserine. We demonstrate that in addition to the heme, the activity of human CBS is influenced by the redox state of the CXXC motif. Interestingly, the activity of CBS responds reciprocally to the oxidation state of the two motifs, increasing when the CXXC motif is reduced while decreasing when the heme is reduced. To resolve this seeming paradox, we have determined the midpoint redox potentials of the heme in full-length human CBS and the CXXC motif and found them to be -356 ± 6 mV and -240 ± 4 mV respectively, versus the standard hydrogen electrode. The reversible formation of a disulfide bridge between C272 and C275 was demonstrated by mass spectrometry, which also revealed the presence of the sulfenic acid intermediate state of the CXXC motif. These studies suggest that the presence of two redox sensors in human CBS can fine tune the response of this protein to the ambient redox state rendering it maximally active in a potential range where the CXXC motif is reduced and the heme is oxidized.

4.2 Introduction

Cystathionine β-synthase (CBS) is a novel pyridoxal 5′-phosphate (PLP)-dependent heme protein that catalyzes the condensation of serine and homocysteine to cystathionine (*1, 2*). CBS has a modular domain structure and consists of an N-terminal domain which houses the PLP and the heme binding sites along with a second redox active CXXC motif. The C-terminal domain of the protein contains a tandem repeat of CBS domains, CBS1 and CBS2, which are believed to be involved in the binding of the allosteric activator, S-adenosylmethionine (AdoMet) (*3*). The full-length enzyme exhibits oligomeric heterogeneity and exists as a mixture of tetramers and higher order oligomers (*4, 5*). Limited proteolysis of human CBS generates a more stable truncated dimeric form missing 143 residues from the C-terminal end and exhibits an ~4 fold higher k_{cat} than the full-length enzyme (*6, 7*). TNFα activation of transformed human liver cells also leads to formation of a truncated CBS dimer demonstrating the physiological relevance of this form of the enzyme (*8*).

CBS is located at a metabolic junction where the decision is made to conserve methionine by salvaging homocysteine to the methionine cycle or to commit it to cysteine, and it is thus subjected to complex regulation (Fig. 1). AdoMet, which signals methionine sufficiency, is a V-type allosteric activator and increases the specific activity of CBS 2- to 3-fold (*9*). AdoMet also stabilizes CBS, increasing the half life of the protein in liver (*10*). The C-terminal domain, to which AdoMet is presumed to bind (*11*), imposes intrasteric inhibition, which is alleviated either by its truncation or by binding of AdoMet (*6, 12, 13*). In addition to these modes of regulation, CBS is also subjected to redox regulation (*14*). Thus, under *in vitro* conditions, changes in the activity of CBS are

correlated with changes in the oxidation state of the heme with the protein being ~2-fold more active under oxidizing conditions. However, the role of the CXXC motif has not been assessed since the high homocysteine concentrations used in the *in vitro* assay (30 mM) would reduce the CXXC disulfide if it existed, and mutations of the cysteines in this motif mimic only the reduced state of the protein (*15*). One rationale for redox regulation of CBS is that this protein, by catalyzing the committing step for cysteine synthesis via the transsulfuration pathway, influences the synthesis of the antioxidant, glutathione (Fig. 1). It is estimated that ~50% of the cysteine incorporated into glutathione in liver originates from the transsulfuration pathway (*16, 17*) while the remainder is presumably derived from extracellular cystine via import and subsequent reduction. The role of CBS in provision of cysteine is evidenced by the lower cysteine concentration in brain and liver in a murine knockout model of hyperhomocysteinemia, heterozygous for CBS gene disruption (*18*).

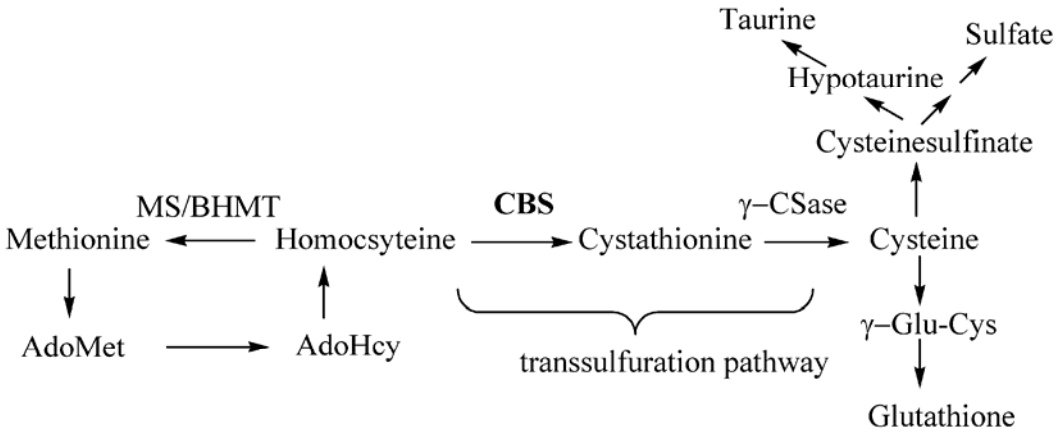

Fig 1. The transsufuration pathway links homocysteine and glutathione metabolism. MS, BHMT and γ-CSase denote methionine synthase, betaine-homocysteine methyltransferase and γ-cystathionase respectively.

The heme in CBS is ~20Å away from the catalytic site where the PLP is bound (Fig. 2) (*15, 19*). The heme resides within an N-terminal extension of ~70 amino acids, which is absent in the closely related yeast enzyme (*20*). CBS binds a single equivalent of heme b per monomer and H65 and C52 serve as the axial ligands in both the ferric and ferrous states (*15, 19*). The heme is not essential for catalysis as evidenced by the retention of ~40 percent of wild-type activity in a hemeless variant of human CBS (*21*). Despite the substantial distance from the active site, changes in the heme environment elicited by binding of exogenous ligands to the heme, or a change in the heme iron's spin or oxidation state, affect CBS activity, consistent with a regulatory role for this cofactor (*22-24*). Ferrous CBS can bind small gaseous molecules like CO and NO (*24*), a property shared by heme sensor proteins viz. FixL, CooA, and HemeAT (*25*). Based on these characteristics, CBS has been postulated to be a redox-regulated heme sensor protein (*15*).

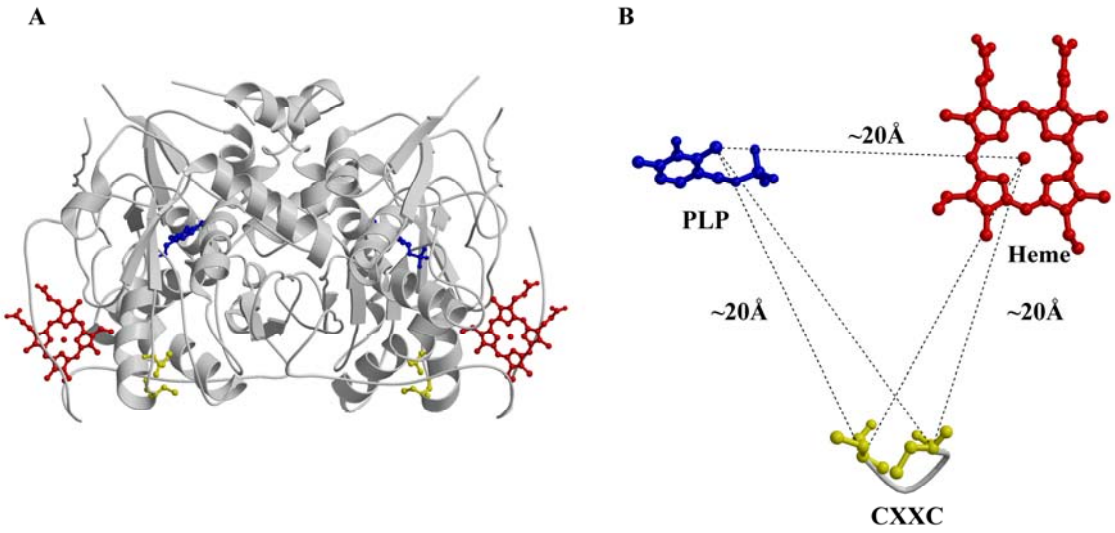

Fig 2. A. Structure of the truncated dimeric form of CBS showing the locations of heme (red), PLP (blue) and the cysteines in the CXXC motif (yellow). B. The relative positions

of the PLP, heme and the CXXC motif in the crystal structure of CBS-ΔC143. The numbers represent approximate distances in Å.

The CXXC motif in CBS is approximately equidistant from the heme and PLP centers being ~20Å away from each (Fig. 2). The CXXC motif is commonly found in the active sites of the thioredoxin family of proteins and is usually involved in thiol-disulfide exchange reactions (*26*). In human CBS, residues C_{272}-P_{273}-G_{274}-C_{275} comprise the CXXC motif, which is conserved in several organisms but is missing in the yeast and *Dictyostelium* enzymes (*1*). It is interesting to note that the CXXC motif in thioredoxin is also comprised of the same sequence of residues i.e., CPGC (*26*). Two crystal structures of the truncated dimer of CBS have been reported and the CXXC motif is in the disulfide-linked state in one and in the dithiol state in the other (*14, 19*). The crystal structures reveal that the CXXC motif is accessible to small molecule reductants, e.g. dithiothreitol, which was used for crystallization of the dithiol form of the enzyme, and suggests that this motif may be redox active in CBS.

In this study, we have characterized the two redox centers in CBS, the heme and the CXXC motif, as a first step towards evaluating their potential for redox regulation in the intracellular milieu. To determine the effect, if any, of the CXXC redox state on CBS activity, we have developed a new assay in which a nonthiol substrate, homoserine, substitutes for homocysteine. We have determined the midpoint potentials for the heme and the CXXC motif in human CBS. Our results suggest that the presence of two redox

sensitive motifs in CBS may allow for fine-tuning of the redox responsiveness of the enzyme to the ambient potential.

4.3 Materials and methods

Materials-Serine, Isopropyl β-D-1-thiogalactopyranoside (IPTG), iodoacetic acid (IAA), dithiotreitol (DTT), methyl viologen, benzyl viologen, anthroquinone 2-sulfonic acid, trypsin and Glu-C (V8-E) were purchased from Sigma. [^{14}C]-Serine (158 mCi/mmol) was purchased from Amersham and GST Sepharose from Pharmacia. Thrombin was purchased from GenTrac Inc., Middleton, WI. Complete tablets (protease cocktail inhibitors) were purchased from Roche Diagnostics (Mannheim, Germany). Rapigest was purchased from Waters (Milford, MA). Mal-PEG 5 kD was purchased from Laysan Bio Inc (Alabama). Mal-PEG 5 kD is usually contaminated with lower molecular weight components that cause smearing during polyacrylamide gel electrophoresis. To avoid this problem, the lower molecular weight contaminants were separated from Mal-PEG 5 kD using a PD-10 desalting column (from Amersham) and 50 mM Tris-HCl buffer, pH 8, for isocratic elution. All the other reagents were used without further purification.

Purification of Full-Length CBS and the Truncated Dimer-The truncated dimer, CBS-ΔC143, lacking the C-terminal 143 amino acids, and the full-length wild-type enzyme were expressed and purified from *Escherichia coli* BL21 cells (Invitrogen) as described previously (*14*) except that reducing agents were omitted from all the steps of the purification.

Homoserine Assay for CBS- This assay is a modification of the standard assay described previously (*14*), where the natural substrate, L-homocysteine, is replaced by the nonthiol derivative, L-homoserine (Fig. 3). The enzyme activity was assayed under aerobic conditions using 30 mM [^{14}C]-serine and 10 mM L-homoserine in the presence or absence of 20 mM DTT or 20 mM glutathione. The amount of enzyme used in the assay was 1 μg for the truncated dimer and 5 μg for full-length CBS. One unit of enzyme activity represents the amount needed for formation of 1 μmol of product•h^{-1} at 37 °C. Protein concentration was determined by the Bradford method using bovine serum albumin as a standard.

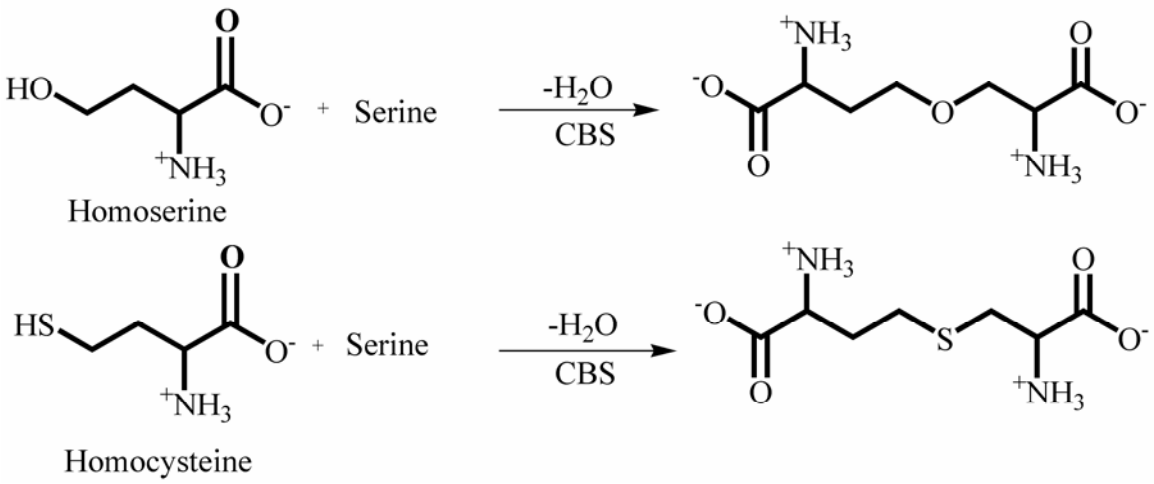

Figure 3. Schematic representation of the condensation reaction between serine and homoserine or the alternate substrate, homoserine, catalyzed by CBS.

Determination of the Redox State of the CXXC Motif by Mass Spectrometry (MS)- CBS-ΔC143 (50 μg) in the reduced (with 50 mM DTT) and oxidized (lacking DTT)

states was treated with IAA (20 mM) for 1 h at room temperature in the dark. Excess DTT was removed from the reduced sample preceding the alkylation step, by extensive washing with 10 mM ammonium bicarbonate buffer, pH 8, containing 8 M urea, using a YM-30 Centricon concentrator (Millipore). The alkylation reaction was quenched by addition of excess DTT and the samples were diluted 10-fold and washed with 10 mM ammonium bicarbonate buffer, pH 8 using a YM-30 Centricon concentrator. Proteolytic digestion was then performed using Glu-C or trypsin at an enzyme to substrate ratio of 1:20 (wt/wt). Rapigest, a mild detergent, was used as per the vendor's instructions, to improve sequence coverage. The digestion reaction was carried out for 30 h at 37°C and the peptides were separated by HPLC on a C18 column (PepMap100, 75 µm x 15 cm, 3-µm 100 Å, LC Packings, Sunnyvale, CA) using a gradient of acetonitrile and water. The solvents used for separation were: A (water with 0.3% formic acid) and B (acetonitrile containing 0.3% formic acid). The gradient was 10-35% solvent B over 20 min at a flow rate of 40 µl/min. The masses of individual peptides were determined by ESI-MS on a Quadrupole time-of-flight mass spectrometer (Applied Biosystems). Peptides were identified by tandem ESI-MS/MS sequencing.

Spectroelectrochemistry of Full-length CBS-Potentiometric measurements were performed using a two-electrode single compartment spectroelectrochemical cell containing a gold foil working electrode and a silver/silver chloride reference electrode (*27*). The experiments were performed under a nitrogen atmosphere in a Belle Technology glove box and in a vacuum atmosphere chamber, with <1 ppm oxygen. Potential measurements are reported relative to the normal hydrogen electrode and were determined in the reductive and oxidative directions. The experiments were carried out at

25°C in 50 mM potassium phosphate buffer, pH 7.2. The potentials were determined in the reductive direction by titrating the enzyme with sodium dithionite (added in increments of 2 μM). The enzyme concentration was maintained at ~10 μM in a 4 ml cell. Methyl viologen (10-20 μM), benzyl viologen (10-20μM) and anthraquinone 2-sulfonic acid (10 μM) were used as the mediator dyes in the potentiometric experiments. The potentials for the indicator dyes are as follows: methyl viologen (E^o = -440 mV, pH 7.5), benzyl viologen (E^o = -360 mV, pH 7.5) and anthraquinone 2-sulfonic acid (E^o = -225 mV, pH 7.0). The system was deemed to be at equilibrium in these experiments when the measured potential change was less than 1 mV in 5 min, and this was typically achieved within 45 min following addition of dithionite. In the oxidative direction, 5 μM aliquots of potassium ferricyanide were added to CBS, previously reduced with 75 μM dithionite. The UV-visible spectra in each experiment were recorded from 300 to 800 nm on a Cary 100 spectrophotometer. The absorbances at 428 nm and 449 nm were used to estimate the amount of oxidized and reduced species, respectively. The final spectra were obtained by subtracting the blank, i.e. spectra of the mediator dyes in the same buffer and at the same potential from the spectrum of the enzyme. The measured potential was fit to the Nernst equation (equation 1), where the concentration of the reduced species at a given potential was obtained by the difference in absorbance at 428 nm or 449 nm from the spectrum of the fully oxidized form (in the reductive direction).

$$E = E + \frac{0.059}{n} \log \frac{[ox]}{[red]} \qquad \text{eq. 1}$$

Alkylation with Mal-PEG and Determination of the Midpoint Potential of the CXXC Motif-Samples of CBS-ΔC143 (50 μg each) in 50 mM Tris-HCl, pH 8, were incubated

with various ratios of oxidized to reduced DTT for 2.5 h at 37°C. Thereafter, samples were precipitated with an equal volume of 20% TCA and centrifuged at 13,500 x *g* for 20 min. The precipitated samples were washed three times with 1 ml of chilled acetone and then dried. The precipitates were resolubilized with 50 mM Tris-HCl, pH 8, 3% SDS, 1 mM EDTA and 5 mM Mal-PEG. The samples were incubated in this buffer for 10 min at 37°C. The reaction was quenched with excess DTT and centrifuged at 13,500 x *g* for 20 min to remove any insoluble protein. The cleared samples were then washed extensively with buffer free of Mal-PEG using YM-30 Centricons (Millipore) to remove excess alkylating reagent. Thereafter, the samples were mixed with gel loading buffer and resolved on a 6% polyacrylamide gel using electrophoresis at 30 mA current. The protein bands were stained with Coomassie blue and the band intensities were estimated with the imaging software installed in the Gel-Doc instrument (BioRad). The midpoint potential was -240 ± 4 mV.

Alkylation with Mal-PEG and Determination of the Midpoint Potential of the CXXC Motif-Samples of CBS-ΔC143 (50 μg each) in 50 mM Tris-HCl, pH 8, were incubated with various ratios of oxidized to reduced DTT for 2.5 h at 37°C. Thereafter, samples were precipitated with an equal volume of 20% TCA and centrifuged at 13,500 x *g* for 20 min. The precipitated samples were washed three times with 1 ml of chilled acetone and then dried. The precipitates were resolubilized with 50 mM Tris-HCl, pH 8, 3% SDS, 1 mM EDTA and 5 mM Mal-PEG. The samples were incubated in this buffer for 10 min at 37°C. The reaction was quenched with excess DTT and centrifuged at 13,500 x *g* for 20 min to remove any insoluble protein. The cleared samples were then washed extensively with buffer free of Mal-PEG using YM-30 Centricons (Millipore) to remove excess

alkylating reagent. Thereafter, the samples were mixed with gel loading buffer and resolved on a 6% polyacrylamide gel using electrophoresis at 30 mA current. The protein bands were stained with coomassie blue and the band intensities were estimated with the imaging software installed in the Gel-Doc instrument (BioRad). The midpoint potential was calculated using equation 2, where $E^{o'}$ = -250 mV, the standard reduction potential for DTT at pH 8 and 37°C, R is the universal gas constant, T is the temperature in

$$E^0 = E^{0'} + \frac{RT}{nF} \ln \frac{[DTT_{red}]}{[DTT_{ox}]} \qquad \text{eq. 2}$$

degrees Kelvin, *F* is the Faraday constant, *n* is the number of electrons transferred and E^o is the redox potential under experimental conditions.

4.4 Results

Purification and redox-dependent CBS activity-The truncated dimer (CBS-ΔC143), and full-length wild-type CBS were obtained in at least 95% purity as determined by SDS-PAGE analysis and by a ratio of ~1 for the 280:428 nm absorbance (not shown). The specific activity of the full-length enzyme and the truncated dimer in the presence of DTT and homoserine, are 18.3 ± 1.0 and 350 ± 13 μmol•h^{-1}•mg^{-1} protein compared to 350 ±40 and 600 ±70 μmol•h^{-1}•mg^{-1} protein respectively in the standard assay with homocysteine. In the absence of DTT, the activity of the truncated dimer and the full-length CBS were 4.6- and 1.6-fold lower respectively (Table 1). Glutathione (20 mM) was less effective at reducing CBS than DTT at least under the assay conditions, and a modest 1.3 fold increase in specific activity was observed with the truncated dimer while no effect was detected with the full-length enzyme, probably due to the low activity associated with the

full-length enzyme in the homoserine assay. Since the oxidized state of the heme iron in CBS is unaffected by DTT as evidenced by the presence of a ferric Soret peak at 428 nm (*14*), these results suggest that the enhancement in activity upon reduction, is due to a change in the redox state of the cysteines.

Due to the low specific activity of full-length CBS seen in the homoserine assay, further kinetic characterization was performed only with the truncated enzyme. The K_{MHser} and K_{MSer} for the truncated dimer are 1.3 ± 0.2 mM and 1.6 ± 0.2 mM, respectively (Table 1). These values are similar to the kinetic parameters reported earlier for the full-length enzyme in the standard assay (K_{Mser} = 2.0 mM K_{MHcy} = 5 mM) (*7, 28*). In contrast, the K_M values for serine and homocysteine reported for the truncated dimer in the standard assay are significantly higher (K_{Mser} =18 mM and K_{MHcys} = 9.7 mM) (*7*). The basis for these differences is not known.

Table 1. Kinetic parameters for the full length and the truncated CBS using homoserine and serine under standard assay conditions

CBS	K_m[a]		Specific Activity[b]		
	Homoserine	Serine	-DTT	+DTT	Fold Activation
Full-length	N.D[c]	N.D[c]	11.4 ± 0.8	18.3 ± 1.0	1.6
CBS-ΔC143	1.3 ± 0.2	1.6 ± 0.2	76.4 ± 5.0	350 ±13.0	4.5

[a] K_M is in units of mM

[b] Specific activity in units of μmoles of cystathionine formed $h^{-1}mg^{-1}$ of protein and was determined in the presence of AdoMet for full-length CBS

[c] Not determined

Detection of a disulfide bond in the CBS CXXC motif by mass spectrometry-Since the truncated variant of CBS does not exhibit the highly heterogenous oligomeric and aggregation states seen with the full-length enzyme, MS analysis for monitoring the redox state of the CXXC motif was conducted on this form of the enzyme. Generation of CBS-ΔC143 leads to deletion of only one of the eleven cysteines present in the full-length enzyme, C431, which is reported to be solvent accessible (*4*). Alkylation of CBS-ΔC143 with IAA in the presence or absence of DTT and subsequent digestion with trypsin or Glu-C led to the identification of all nine peptides in which the ten cysteine residues in the truncated dimer reside. The masses of the individual peptides were determined by ESI TOF MS (Table 2) and MS/MS fragmentation pattern of each peptide was used to confirm its identity. One peptide carried the two cysteines in the CXXC motif. Under reducing and non-reducing conditions, the masses of all but one peptide exhibited modification of the resident cysteine by a single IAA residue i.e., an addition of 58 Da. The exception was the peptide, $KC_{272}PGC_{275}$RIIGVDPE, which exhibited a monoisotopic mass of 1501.69 (corresponding to the addition of two IAA residues), under reducing conditions and a monoisotopic mass of 1383.66 (corresponding to the presence of an intramolecular disulfide bridge) under air oxidized conditions. The +3 charge states of the two forms of the peptide are shown in Fig. 4 with m/z values of 501.57 and 462.22 for the reduced and oxidized states respectively.

Table 2. Comparison of the expected and observed monoisotopic masses of CBS peptide fragments with IAA–modified cysteines

Cysteine Residue	Peptide Covering the Cysteine	Molecular Weight[a]		Number of IAA Modifications	
		Observed	Calculated	-DTT[b]	+DTT[c]
52	CTWLGRPASESPHHHTAPAK	2368.05	2368.11	1	1
15	VGPTGCPHRSGPHSAKGSLE	2030.92	2030.96	1	1
103	FGLKCELLAK	1178.60	1178.64	1	1
109	CEFFNAGGSVK	1215.45	1215.52	1	1
346	MLIAQEGLLCGGSAGSTVAVAVK	2232.09	2232.15	1	1
370	CVVILPDSVR	1157.57	1157.61	1	1
165	CIIVMPEK	989.42	989.49	1	1
272, 275	KCPGCRIIGVDPE	1501.63	1501.69	0	2
244	ILQQCDGKLDMLVASVGTGGTITGIARKL	3272.71	3272.75	1	1

[a]in Da

[b]Sample was modified with IAA without reduction

[c]Sample was reduced with DTT before IAA modification

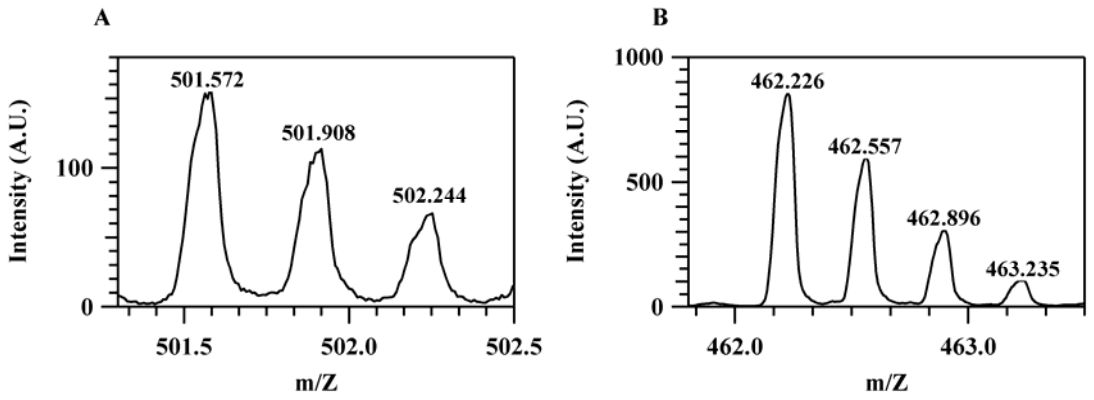

Figure 4. A. Mass analysis of the $KC_{272}PGC_{275}$RIIGVDPE peptide obtained by two IAA modifications (under reducing conditions). The charge state is +3 and yields an *M*r of 1501.69 and an m/z value of 501.57. B. Mass analysis of the $KC_{272}PGC_{275}$RIIGVDPE peptide containing a disulfide bridge between C272 and C275 (under air oxidized conditions). The charge state is +3 and yields an *M*r of 1383.66 and an m/z value of 462.2.

Evidence for the presence of a sulfenic acid in the CXXC motif-MS analysis of the peptides generated under air oxidized conditions revealed a species with a +4 charge state corresponding to an m/Z value of 365.937 as shown in Fig. 5. The monoisotopic mass of this peptide is 1459.72 and represents the presence of a 59 Da and a 17 Da modification corresponding to the addition of a single IAA and a hydroxyl group respectively, to 1383.66, the mass of the $KC_{272}PGC_{275}$RIIGVDPE peptide bearing a disulfide bond. The presence of a hydroxyl group is consistent with the formation of a sulfenic acid

modification representing an intermediate between the dithiol and disulfide states, in which one cysteine is oxidized to sulfenic acid and the other is reduced.

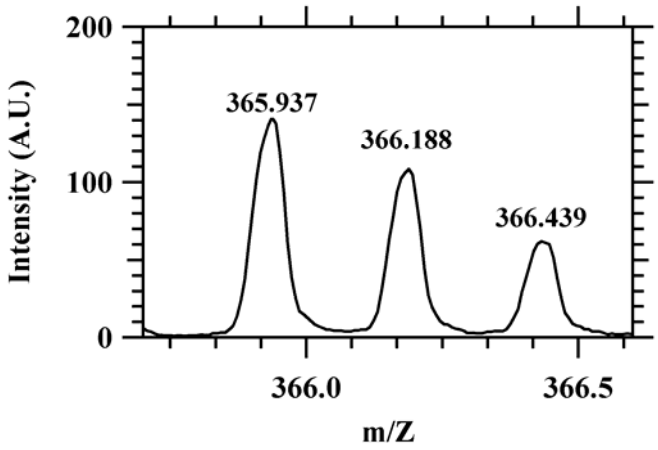

Figure 5. Mass analysis of the $KC_{272}PGC_{275}$RIIGVDPE peptide bearing a sulfenic acid derivative on one of the cysteines in the CXXC motif. The charge state is +4 and yields an *M*r of 1459.66 and an m/z value of 365.9.

Determination of the midpoint potential of the CXXC center in CBS-Although Mal-PEG 5 kD has a molecular mass of 5 kD it causes an ~20 kD shift per modified thiol in the electrophoretic mobility of polypeptides under denaturing conditions (*29*). When CBS-ΔC143 was alkylated with Mal-PEG at varying ratios of oxidized to reduced DTT, two bands of 245 and 205 kD molecular mass were observed (Fig. 6). The band with a molecular mass of 245 kD represents the addition of 200 kD to the mass of CBS-ΔC143 (45 kD) and corresponds to the presence of ten Mal-PEG moieties. The lower protein band at ~205 kD corresponds to the oxidized population of CBS bearing eight Mal-PEG

modifications, consistent with the presence of two cysteines in a disulfide linkage. The intensity of the higher molecular mass band decreased with a corresponding increase in the intensity of the lower band as the ratio of reduced to oxidized DTT decreased (Fig. 6). Quantitative analysis of the band intensities as a function of the redox potential poised by varying ratios of oxidized to reduced DTT, yielded an estimated midpoint potential of -240 ± 4 mV for the CXXC motif in CBS.

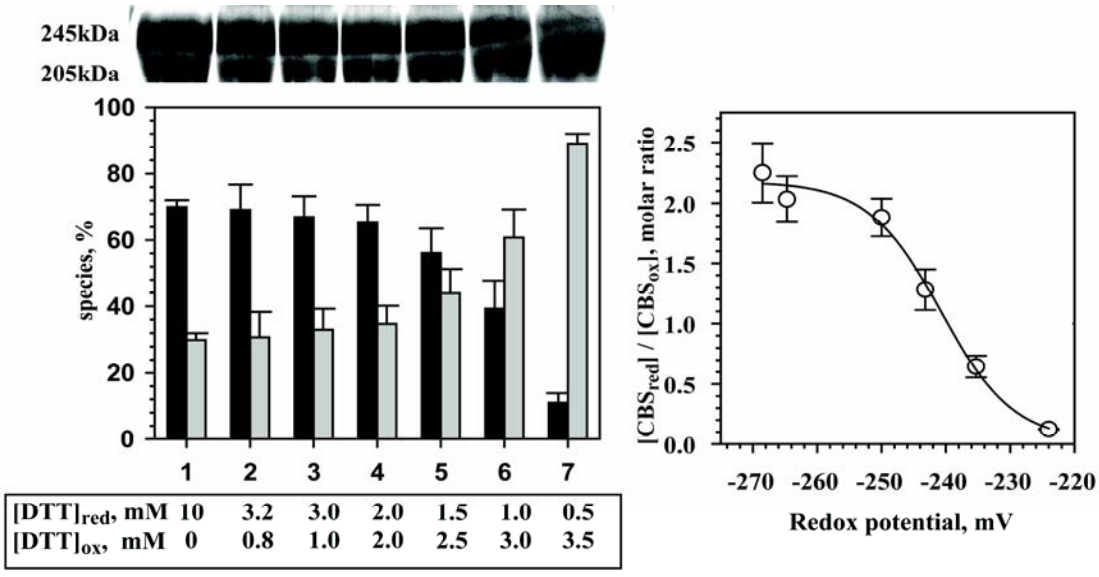

Figure 6: Determination of the midpoint potential of the CXXC motif by alkylation with Mal-PEG. A. Distribution of the upper and lower bands representing the reduced and oxidized forms of CBS-ΔC143 respectively by SDS PAGE analysis. The upper band results from two extra MAL-PEG modifications versus the population representing the lower band. The relative intensities of the upper and lower bands depend on the ratio of DTT_{red}/DTT_{ox}. (B) Quantitative analysis of the data shown in A. The chart at the bottom indicates the relative amounts of oxidized and reduced DTT in each reaction mixture. (C)

Nernst analysis of the CXXC redox state at varying potentials poised by changing the relative proportions of reduced and oxidized DTT.

Determination of the midpoint potential of the heme center in full-length CBS- Spectroelectrochemical titrations were performed to estimate the redox potential of the heme in full-length CBS by following the intensity of the heme Soret peak as described under Methods. From this analysis, the average midpoint potential for the heme in wild type full-length CBS was determined to be -356 ± 6 mV for titrations in the reductive (average = -353 ± 6 mV) and oxidative directions (-358 ± 5 mV). Fig. 7 shows a representative potentiometric titration of the heme in full-length CBS. The presence of 100 μM AdoMet, an allosteric activator of CBS, during the titration had no effect on the heme redox potential.

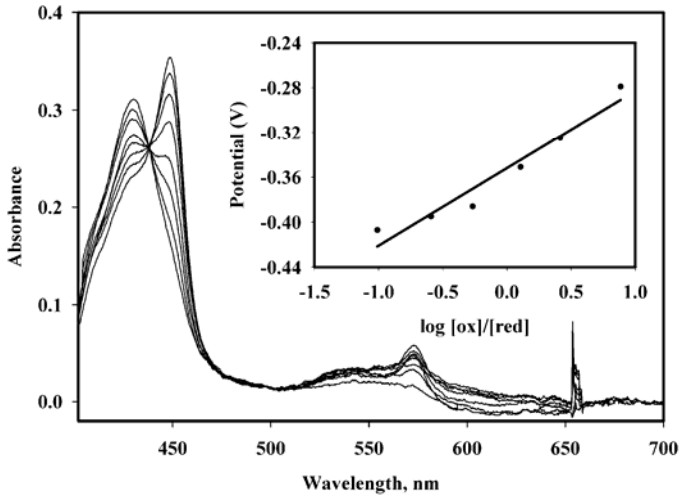

Figure 7. Redox potential determination for the heme in full-length CBS. The potentiometric titration was performed at 25˚C in the presence of 20 μM benzyl viologen, 20 μM methyl viologen, 8 μM wild type CBS with 2 μM incremental addition of sodium dithionite. The spectra are shown after mediator dye subtraction. The 428 nm ferric species converted to the 449 nm ferrous species as sodium dithionite was added. *Inset*. Nernst analysis of this data yielded a redox potential of -352 ± 4 mV for the heme with a slope of 73 ± 7.5 mV.(Madzelan, P Banerjee R)

4.5 Discussion

CBS catalyzes the first step in the transsulfuration pathway, which converts homocysteine to cysteine via the intermediate formation of cystathionine (Fig. 1). The quantitative significance of this pathway for provision of intracellular cysteine, needed for glutathione synthesis, links the metabolism of homocysteine directly to cellular redox homeostasis (*16, 17*). Additionally, the activity of CBS contributes to determining the balance between the transsulfuration and transmethylation pathways for clearing intracellular homocysteine and thereby determining the fate of intracellular sulfur in mammals. As expected, this critical junction in sulfur metabolism is subject to multiple layers of regulation including regulation by AdoMet and by the ambient redox state (*1*).

Cell culture studies have revealed that under conditions of oxidative stress, the flux of homocysteine through the transsulfuration pathway is increased (*17*). The physiological rationale for this response is that it represents an auto corrective reaction that, by

increasing synthesis of cysteine stimulates synthesis of glutathione, thereby replenishing the antioxidant pool, which is depleted under oxidizing conditions. The mechanism of up-regulation of the transsulfuration flux is however, not known. Studies with purified recombinant human CBS have revealed that the enzyme is approximately two-fold less active when low potential reductants viz. titanium citrate or dithionite are added to the standard assay mixture (*14*). Furthermore, this change in activity is correlated with a change in the redox state of the heme from the ferric to the ferrous state (*14*) and is unaffected by mutation of either cysteine in the CXXC motif (*15*). These observations support our earlier conclusion that under the conditions of the in vitro assay, the heme rather than the CXXC motif in CBS, is the redox sensor (*15*). However, the role of the CXXC motif in redox regulation of CBS cannot be assessed in this assay for the following reason. One of the substrates of CBS, homocysteine, is itself a thiol and, at the high concentrations that it is present in the standard reaction mixture (30 mM), would reduce the CXXC disulfide. Hence, under the standard assay conditions, the CXXC motif is in the reduced state, and only redox regulation by the heme can be interrogated. Mutation of the cysteines in the CXXC motif mimics the reduced dithiol state of this motif, and the resulting mutants are expected to retain heme-dependent redox sensitivity, as reported (*15*). Hence, the influence of the CXXC redox state on the activity of CBS has not been previously addressed and, in the absence of the values for the midpoint potentials for the two redox centers in CBS, their physiological relevance to redox responsiveness, has not been evaluated.

To address these gaps in our understanding of the redox regulation of CBS, we have developed a new assay for the enzyme that uses the hydroxo-derivative of homocysteine,

homoserine (Fig. 3). Despite the significant difference in the pKa of the thiol group in homocysteine (~10.8) versus homoserine (~15), only a 19-fold lower activity is seen with the full-length enzyme when homoserine replaces homocysteine in the assay (18.3 ± 1.0 versus 350 ± 40 μmol•h^{-1}•mg $protein^{-1}$). This suggests that deprotonation of homocysteine for the β-replacement reaction, is not completely rate limiting. With the truncated dimeric CBS, an even smaller 1.7-fold difference is observed between the two substrates (350 ± 13 versus 600 ±70 μmol•h^{-1}•mg $protein^{-1}$). Both forms of the enzyme however exhibit higher activity in the homoserine assay in the presence of DTT, indicating that the dithiol form of the CXXC motif in CBS is associated with more active enzyme.

MS analysis was employed to verify the difference in the oxidation state of the CXXC motif suggested by the difference in the enzyme activity assays in the presence and absence of DTT. A combination of trypsin and Glu-C resulted in the recovery of all nine peptides harboring the ten cysteine residues in the truncated form of CBS, and confirmed the presence of a disulfide bond in the CXXC motif in the protein as isolated and its reduction in DTT-treated samples (Table 2 and Fig. 4).

Reversible cysteine-targeted oxidative modifications such as formation of intramolecular disulfides, is a common strategy for regulating proteins under oxidative stress conditions (*30*). An example of a PLP-dependent enzyme that is subject to such regulation is human mitochondrial branched chain aminotransferase (*31*). The latter, like CBS, contains a regulatory CXXC motif involving cysteines 315 and 318. In the C318A mutant of the branched chain aminotransferase, C315 was shown to form a sulfenic acid intermediate, suggesting that this is the reactive cysteine that is initially oxidized during

formation of the disulfide bond. We also detected a sulfenic acid intermediate in CBS by mass spectrometry (Fig. 5). In the protein as isolated, this species is present at low abundance as suggested by the relatively low intensity associated with this signal, which precluded assignment by MS/MS analysis of the particular cysteine in the CXXC motif that is oxidized to sulfenic acid. The instability of the previously reported C272A or C275A mutants of CBS (*15*) has similarly limited efforts to identify the reactive (versus resolving) cysteine in the CXXC motif.

Disulfide bonds have traditionally been considered to be either catalytic or structural in function. There is however growing recognition of a third class of disulfides, the allosteric disulfide bonds, which are capable of controlling protein function by triggering a conformational change. A recent analysis of protein crystal structures has revealed differences in disulfide bond geometry and in disulfide strain energy between structural, catalytic and allosteric disulfide bonds (*32*). Disulfides with low dihedral strain energies, typically between 9.7-10.4 kJ mol^{-1} are assigned to be structural in nature whereas those with higher values are assigned as either catalytic or allosteric in function ($\geq$ 12 kJ mol^{-1}), with the catalytic disulfides typically having higher values than the allosteric ones (*32*). Based on this analysis, the C272-C275 disulfide bond in CBS is classified as a -/+RHHook catalytic bond of the type seen in oxidoreductases (e.g. thioredoxin) and isomerases (e.g. protein disulfide isomerase) rather than an allosteric disulfide bond, which have the –RHStaple configuration (*32*). The estimated dihedral strain energy of the disulfide bond in the structure of truncated CBS (PDB 1JBQ) is 15.95 kJ mol^{-1}, which also places it in the category of catalytic disulfides. However, given the distance between the C272-C275 bond and the active site (Fig. 2), it appears unlikely that these residues

play a catalytic role, nor is this warranted based on the PLP-dependent β-replacement chemistry of the reaction. In addition, mutation of the cysteines in the CXXC motif results in retention of enzyme activity (*15*), excluding an essential role for these residues in catalysis. It is possible however that the CXXC motif in CBS may be involved in interactions with and/or regulation of other proteins. It is important to note however that while the CXXC motif appears to be relatively surface exposed in the structures of the truncated CBS dimer (*15, 19*), its accessibility in the full-length protein is not known.

The CXXC motif in CBS sequences is generally correlated with the presence of the putative heme ligands and suggests that they may both function in a regulatory capacity (*1*). In fact, the eleven cysteine residues found in human CBS are highly conserved across other mammalian CBSs. In the native full-length human protein, only two cysteines are reported to be readily solvent accessible, C15 in the heme domain and C431 in the regulatory domain (*4*). However, the highly heterogeneous oligomeric state of purified recombinant human CBS, even in the presence of DTT, substrates or AdoMet (unpublished observations), limits such analysis.

The opposing effects of the oxidation states of the two redox centers on the activity of CBS, i.e. activation by reduction of the disulfide and oxidation of the heme, seems at first glance, to be paradoxical. However, inspection of the predicted dependence of CBS activity on the ambient redox potential (Fig 8), reveals that the presence of these two centers can fine-tune its responsiveness to redox changes. The cytoplasmic redox potential is poised by the glutathione, NADPH, dihydrolipoamide and thioredoxin redox couples. In mammalian cells, this value has been estimated to be ~-315 to -325 mV (*33*). The thiol/disulfide redox couple in CBS has a midpoint potential of -240 mV and under

physiological conditions the CXXC motif is likely to be predominantly reduced. In contrast, the heme has a lower midpoint potential of -356 mV, which is similar to values reported for other heme-thiolate proteins such as cytochrome P450 (-360 mV) (*34*), nitric oxide synthase (-347 mV) (*35*), and CooA (-320 mV) (*36*). We note that we have also determined the redox potential of the heme in the truncated dimeric form of CBS and found it to be -287 ± 2 mV (*37*). The difference in redox potential from the value measured for the full-length enzyme in this study, likely derives from changes in the heme microenvironment and/or heme solvent exposure between the two enzyme forms. The heme in full-length CBS is expected to exist as a mixture of the ferric and ferrous states under physiological conditions. Under oxidative stress conditions, an increase in the proportion of the oxidized heme would be primarily responsible for an increase in CBS activity (Fig. 8).

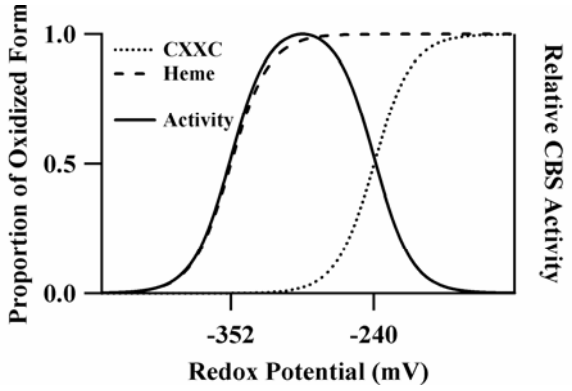

Figure 8. Schematic representation of the relative change in CBS activity with redox potential.

We note however, that varying estimates for the ambient cytoplasmic redox potential have been reported in the literature. Based on the ratio of reduced to oxidized glutathione, values ranging from -200 to -240 mV have been reported (*38, 39*). A similar value for the intracellular potential in *E. coli* (-259 mV) has been reported using a green fluorescent protein-based sensor responsive to the glutathione/glutathione disulfide redox couple (*40*). These higher values predict a different distribution of the oxidized and reduced forms of the heme and CXXC centers under normoxic conditions and activation of CBS would be expected under conditions that shift the redox potential to be more reducing rather than oxidizing (Fig. 8), which is not observed in mammalian cells (*17*).

Another example of a protein whose activity is modulated both by the oxidation state of its heme and by an intramolecular disulfide/dithol equilibrium is neuroglobin (*41*). The heme in neuroglobin is hexacoordinate with bis-histidine axial ligands. Binding of oxygen to the heme therefore depends on the histidine dissociation rate as well as the relative association rates of oxygen and the competing distal histidine ligand. Reduction of the disulfide bond in neuroglobin results in a significant decrease in oxygen affinity, which in turn results from a decrease in the dissociation rate of the histidine. It is not known to what extent the redox state of the CXXC motif in CBS influences the reactivity of the heme to exogenous ligands.

The thiol versus disulfide state of a protein can have other functional consequences. For instance, the nuclear localization of the redox sensitive YAP1 transcription factor is triggered by reduction of a regulatory disulfide, which exposes the nuclear localization signal (*42*). We have recently reported that CBS is a target of sumoylation and that it localizes to the nucleus in addition to its well known cytoplasmic residence (*43*). The role

of CBS inside the nucleus or the mechanism of its import into this compartment is not known. It is also not known whether the redox state of the CXXC motif has any influence on the nuclear function and/or localization of CBS.

In summary, we report that in addition to the oxidation state of the heme, the redox state of the CXXC motif potentially serves as another switch for fine-tuning the redox responsiveness of the enzyme. The midpoint potentials of the heme and CXXC centers in human CBS reported in this study allows prediction of how the activity of this enzyme may be modulated by changes in the ambient intracellular redox potential.

Acknowledgments

I thank Peter Madzelan and for his contribution in detecting the midpoint potential of the heme in full-length CBS.

References

1. Banerjee, R., and Zou, C. G. (2005) Redox regulation and reaction mechanism of human cystathionine-beta-synthase: a PLP-dependent hemesensor protein. *Arch Biochem Biophys 433*, 144-56.
2. Singh, S., Madzelan, P., and Banerjee, R. (2007) Properties of an unusual heme cofactor in PLP-dependent cystathionine beta-synthase. Nat. Prod. Rep. 24, 631-39.

3. Bateman, A. (1997) The structure of a domain common to archaebacteria and the homocystinuria disease protein. *Trends Biochem. Sci. 22*, 12-13.

4. Frank, N., Kery, V., Maclean, K. N., and Kraus, J. P. (2006) Solvent-accessible cysteines in human cystathionine beta-synthase:Crucial role of cysteine 431 in S-adenosyl L-methionine binding. *Biochemistry 45*, 11021-11029.

5. Sen, S., and Banerjee, R. (2007) A Pathogenic Linked Mutation in the Catalytic Core of Human Cystathionine beta-Synthase Disrupts Allosteric Regulation and Allows Kinetic Characterization of a Full-Length Dimer. *Biochemistry 46*, 4110-6.

6. Kery, V., Poneleit, L., and Kraus, J. P. (1998) Trypsin cleavage of human cystathionine beta-synthase into an evolutionarily conserved active core: structural and functional consequences. *Arch Biochem Biophys 355*, 222-32.

7. Taoka, S., Widjaja, L., and Banerjee, R. (1999) Assignment of enzymatic functions to specific regions of the PLP-dependent heme protein cystathionine beta-synthase. *Biochemistry 38*, 13155-61.

8. Zou, C.-G., and Banerjee, R. (2003) Tumor necrosis factor-a-induced targeted proteolysis of cystathionine beta-synthase modulates redox homeostasis. *J. Biol. Chem. 278*, 16802-16808.

9. Taoka, S., Widjaja, L., and Banerjee, R. (1999) Assignment of enzymatic functions to specific regions of the PLP-dependent hemeprotein cystathionine b-synthase. *Biochemistry 38*, 13155-13161.

10. Prudova, A., Bauman, Z., Braun, A., Vitvitsky, V., Lu, S. C., and Banerjee, R. (2006) S-adenosylmethionine stabilizes cystathionine beta-synthase and modulates redox capacity. *Proc Natl Acad Sci U S A 103*, 6489-94.

11. Scott, J. W., Hawley, S. A., Green, K. A., Anis, M., Stewart, G., Scullion, G. A., Norman, D. G., and Hardie, D. G. (2004) CBS domains form energy-sensing modules whose binding of adenosine ligands is disrupted by disease mutations. *J Clin Invest 113*, 274-84.

12. Shan, X., Dunbrack, R. L., Jr., Christopher, S. A., and Kruger, W. D. (2001) Mutations in the regulatory domain of cystathionine beta synthase can functionally suppress patient-derived mutations in cis. *Hum Mol Genet 10*, 635-43.

13. Evande, R., Boers, G. H. J., Blom, H. J., and Banerjee, R. (2002) Alleviation of Intrasteric Inhibition by the Pathogenic Activation Domain Mutation, D444N, in Human Cystathionine beta-synthase. *Biochemistry 41*, 11832 - 11837.

14. Taoka, S., Ohja, S., Shan, X., Kruger, W. D., and Banerjee, R. (1998) Evidence for heme-mediated redox regulation of human cystathionine beta-synthase activity. *J Biol Chem 273*, 25179-84.

15. Taoka, S., Lepore, B. W., Kabil, O., Ojha, S., Ringe, D., and Banerjee, R. (2002) Human cystathionine beta-synthase is a heme sensor protein. Evidence that the redox sensor is heme and not the vicinal cysteines in the CXXC motif seen in the crystal structure of the truncated enzyme. *Biochemistry 41*, 10454-61.

16. Beatty, P. W., and Reed, D. J. (1980) Involvement of the cystathionine pathway in the biosynthesis of glutathione by isolated rat hepatocytes. *Arch. Biochem. Biophys. 204*, 80-87.

17. Mosharov, E., Cranford, M. R., and Banerjee, R. (2000) The quantitatively important relationship between homocysteine metabolism and glutathione

synthesis by the transsulfuration pathway and its regulation by redox changes. *Biochemistry 39*, 13005-11.

18. Vitvitsky, V., Dayal, S., Stabler, S., Zhou, Y., Wang, H., Lentz, S. R., and Banerjee, R. (2004) Perturbations in homocysteine-linked redox homeostasis in a murine model for hyperhomocysteinemia. *Am J Physiol Regul Integr Comp Physiol 287*, R39-46.
19. Meier, M., Janosik, M., Kery, V., Kraus, J. P., and Burkhard, P. (2001) Structure of human cystathionine beta-synthase: a unique pyridoxal 5'- phosphate-dependent heme protein. *EMBO J 20*, 3910-6.
20. Jhee, K. H., McPhie, P., and Miles, E. W. (2000) Yeast cystathionine beta-synthase is a pyridoxal phosphate enzyme but, unlike the human enzyme, Is not a heme protein. *J Biol Chem 275*, 11541-4.
21. Evande, R., Ojha, S., and Banerjee, R. (2004) Visualization of PLP-bound intermediates in hemeless variants of human cystathionine beta-synthase: evidence that lysine 119 is a general base. *Arch Biochem Biophys 427*, 188-96.
22. Taoka, S., West, M., and Banerjee, R. (1999) Characterization of the heme and pyridoxal phosphate cofactors of human cystathionine beta synthase reveals nonequivalent active sites. *Biochemistry 38*, 2738-2744.
23. Taoka, S., Green, E. L., Loehr, T. M., and Banerjee, R. (2001) Mercuric Chloride-Induced Spin or Ligation State Changes in Ferric or Ferrous Human Cystathionine b-synthase Inhibit Enzyme Activity. *J. Inorg. Bioc. 87*, 253-259.

24. Taoka, S., and Banerjee, R. (2001) Activity of human cystathionine beta synthase is regulated by CO and NO: Possible role for the hemeprotein in CO sensing. *J. Inorg. Bioc. 87*, 245-251.

25. Gilles-Gonzalez, M. A., and Gonzalez, G. (2005) Heme-based sensors: defining characteristics, recent developments, and regulatory hypotheses. *J Inorg Biochem 99*, 1-22.

26. Holmgren, A., Soderberg, B. O., Eklund, H., and Branden, C. I. (1975) Three-dimensional structure of Escherichia coli thioredoxin-S2 to 2.8 A resolution. *Proc Natl Acad Sci U S A 72*, 2305-9.

27. Dutton, P. L. (1978) Redox potentiometry: determination of midpoint potentials of oxidation-reduction components of biological electron-transfer systems. *Methods Enzymol 54*, 411-35.

28. Kraus, J., Packman, S., Fowler, B., and Rosenberg, L. E. (1978) Purification and properties of cystathionine beta-synthase from human liver. Evidence for identical subunits. *J Biol Chem 253*, 6523-8.

29. Wilkinson, B., Xiao, R., and Gilbert, H. F. (2005) A structural disulfide of yeast protein-disulfide isomerase destabilizes the active site disulfide of the N-terminal thioredoxin domain. *J Biol Chem 280*, 11483-7.

30. Gitler, C., Zarmi, B., and Kalef, E. (1997) General method to identify and enrich vicinal thiol proteins present in intact cells in the oxidized, disulfide state. *Anal Biochem 252*, 48-55.

31. Conway, M. E., Poole, L. B., and Hutson, S. M. (2004) Roles for cysteine residues in the regulatory CXXC motif of human mitochondrial branched chain aminotransferase enzyme. *Biochemistry 43*, 7356-64.

32. Schmidt, B., Ho, L., and Hogg, P. J. (2006) Allosteric Disulfide Bonds. *Biochemistry 45*, 7429-7433.

33. Dooley, C. T., Dore, T. M., Hanson, G. T., Jackson, W. C., S.J., R., and Tsien, R. Y. (2004) Imaging dynamic redox changes in mammalian cells with green fluorescent protein indicators. J. Biol. Chem. 279, 22284-93.

34. Huang, Y. Y., Hara, T., Sligar, S., Coon, M. J., and Kimura, T. (1986) Thermodynamic properties of oxidation-reduction reactions of bacterial, microsomal, and mitochondrial cytochromes P-450: an entropy-enthalpy compensation effect. *Biochemistry 25*, 1390-4.

35. Noble, M. A., Munro, A. W., Rivers, S. L., Robledo, L., Daff, S. N., Yellowlees, L. J., Shimizu, T., Sagami, I., Guillemette, J. G., and Chapman, S. K. (1999) Potentiometric analysis of the flavin cofactors of neuronal nitric oxide synthase. *Biochemistry 38*, 16413-8.

36. Nakajima, H., Honma, Y., Tawara, T., Kato, T., Park, S. Y., Miyatake, H., Shiro, Y., and Aono, S. (2001) Redox properties and coordination structure of the heme in the co-sensing transcriptional activator CooA. *J Biol Chem 276*, 7055-61.

37. Carballal, S., Madzelan, P., Zinola, C. F., Grana, M., Radi, R., Banerjee, R., and Alvarez, B. (2007) Dioxygen reactivity and heme redox potential of truncated human cystathionine beta-synthase. *submitted for publication*.

38. Hwang, C., Lodish, H. F., and Sinskey, A. J. (1995) Measurement of glutathione redox state in cytosol and secretory pathway of cultured cells. *Methods Enzymol. 251*, 212-221.

39. Schafer, F. Q., and Buettner, G. R. (2001) Redox environment of the cell as viewed through the redox state of the glutathione disulfide/glutathione couple. *Free Radic Biol Med 30*, 1191-212.

40. Ostergaard, H., Henriksen, A., Hansen, F. G., and Winther, J. R. (2001) Shedding light on disulfide bond formation: engineering a redox switch in green fluorescent protein. *Embo J 20*, 5853-62.

41. Hamdane, D., Kiger, L., Dewilde, S., Green, B. N., Pesce, A., Uzan, J., Burmester, T., Hankeln, T., Bolognesi, M., Moens, L., and Marden, M. C. (2004) Coupling of the heme and an internal disulfide bond in human neuroglobin. *Micron 35*, 59-62.

42. Kuge, S., Jones, N., and Nomoto, A. (1997) Regulation of yAP-1 nuclear localization in response to oxidative stress. *EMBO J 16*, 1710-20.

43. Kabil, O., Zhou, Y., and Banerjee, R. (2006) Human cystathionine beta-synthase is a target for sumoylation. *Biochemistry 45*, 13528-36.

Chapter 5

Summary and future directions

Summary

CBS is the first enzyme in the transsulfuration pathway which commits homocysteine to cysteine synthesis and is subject to complex regulation. Although it was known that CBS undergoes intrasteric and allosteric regulation, insights into the structural basis of this regulation were obtained for the first time in this study. In addition, this thesis elucidated the role of the CXXC motif and established its redox-dependent role in regulating CBS.

The first part of this dissertation sheds light on localizing conformational changes associated with allosteric and intrasteric regulation of human CBS. CBS functions at a critical metabolic junction where the decision to conserve homocysteine via the methionine cycle or to commit it to transsulfuration and therefore cysteine synthesis is made. It is thus expected that the enzyme is tightly regulated. This includes intrasteric inhibition imposed by the C-terminal domain and allosteric regulation by AdoMet. Interestingly, a subset of pathogenic CBS mutations have been reported that map to the regulatory domain, display a higher level of basal activity but are nonresponsive to allosteric activation. The structural basis for this apparently paradoxical phenotype has been investigated for the first time in this study.

Kinetic studies indicate that the wild-type enzyme equilibrates between at least two conformations, the “basal” state and the “activated state” that is induced by AdoMet. We employed H/D exchange MS to localize focal conformational changes in wild-type CBS induced by AdoMet, to a peptide which spans residues 511-531 in the regulatory domain. We surmise that this region becomes more exposed to solvent in the presence of AdoMet. Interestingly this “activated” conformation is mimicked by the pathogenic mutation

D444N, which has a k_{cat} similar to that of the "activated" state of the wild-type enzyme but is nonresponsive to AdoMet. Interestingly the 511-531 peptide is located in the C-terminal module of the enzyme where AdoMet is predicted to bind. This domain comprises a tandem repeat of two CBS domains. Since the structure of the full-length CBS is unavailable, we have generated a homology modeled structure of the C-terminal regulatory domain using the coordinates for a CBS domain protein from *M.thermoautotrophicus*. The sensitivity of the 511-531 peptide could be consequential of its proximity to the binding site for AdoMet and/or its location on the pathway of allosteric signal transduction.

The kinetics of hydrogen exchange further revealed two surfaces represented by peptides 356-370 and 371-385, which are sensitive to deletion of the regulatory domain. Interestingly several pathogenic mutations including R369C/H and K384N/E have been reported in these two stretches. We have employed the H/D exchange MS data in conjunction with the reported properties of CBS guide our docking model for the full-length enzyme. We reasoned, based on biochemical data that the 356-370 peptide is involved in making direct contact with the regulatory domain and hence maps on to the regulatory-catalytic interface. The 371-385 peptide on the other hand is located at the bottom of a cavity and leads to a short helix leading to a loop representing the C-terminus of the catalytic domain. We employed the docked model of the full-length dimeric CBS to generate a model of the full-length tetramer. in the absence of a full-length crystal structure, this model has been used to rationalize the pathological basis of several patient mutants.

The second part of this dissertation describes the characterization of the linked P78R/K102N pathogenic mutation in the catalytic core of CBS. The mutants P78R and K102N were created to study the contributions of each locus to the linked mutant. The P78R mutant which existed as a mixture of a full-length dimeric form and higher order oligomers, allowed for the first time limited kinetic characterization of the full-length dimeric state of CBS. Upon activation at 4°C, the higher order oligomers converted to the apparently more stable full-length dimer exhibiting a different specific activity. These results suggest the possibility that CBS may distribute itself into various oligomeric states under specific cellular conditions and/or in different compartments and that this may represent yet another mode of regulation.

The unresponsiveness of the P78R/K102N mutant towards AdoMet makes it the first catalytic core mutation reported with such a phenotype. H/D exchange studies conformed that the double mutant exhibited a similar conformation as seen in the D444N mutant indicating that it is also locked in kinetically "activated" state. The finding of AdoMet nonresponsive mutants in both the catalytic as well as the regulatory domains is consistent with the interactions between the two domains.

The third and the final portion of this thesis focused on redox regulation of CBS. For the first time it was established that the CXXC motif in CBS is redox active. The change in the redox state of the CXXC motif is communicated to the catalytic center which causes an increase in activity (4.5-fold in the truncated dimer and 1.6-fold in the full-length enzyme), upon reduction of the disulfide to a dithiol. This modulation in the activity with respect to the redox changes at the CXXC center is opposite to that seen at the heme center where a reduction of the iron actually decreased the activity by ~2 fold.

The reciprocal redox dependency associated with the two centers would represent a mechanism for fine tuning the global redox regulation of CBS. The midpoint potentials of the heme (-356 ± 6mV) and the CXXC center (-240 ± 4mV) reported in this study allows prediction of how CBS activity may be modulated by changes in the ambient redox potential.

Future directions

The physiological relevance of the existence of CBS in various oligomeric forms is yet to be established. Characterization of various mutants have revealed the existence of a mixture of higher order oligomers (including tetramers) and full-length dimers such as seen in the P78R mutant as detected in this thesis. It would be interesting to study the oligomeric distribution of CBS *in vivo*, to assess whether the sampling of different oligomeric states is seen and if it changes under different conditions i.e. oxidative stress or methionine restriction. Investigations to detect the oligomeric state of CBS in the different cellular compartments where it localizes (i.e. in nucleus and the cytoplasm), may further shed light on its diverse functioning.

An important area that can also be further developed, is redox regulation of CBS. *In vitro* studies have identified the redox regulatory centers in CBS. As a next step, the redox status of the enzyme will have to be established *in vivo*. It would be interesting to study the redox status of this enzyme both in the cytoplasm and nucleus. Investigations should be concluded to assess if localization of CBS and/or its function in the nucleus is redox dependent.

Although a change in the redox state in the CXXC motif in CBS has been shown to be communicated to the active site, the mechanism of this transmission is yet to be investigated. Studies aimed at mapping conformational changes if any, or interaction with potential redox partners via the CXXC center will address important gaps in our knowledge of redox regulation of CBS *in vivo*.